CLM-P765

CLM-P765

UKAEA

Preprint

RELAXATION AND MAGNETIC RECONNECTION IN PLASMAS

J. B. TAYLOR

CULHAM LABORATORY
Abingdon, Oxfordshire
1985

CLM-P765

RELAXATION AND MAGNETIC RECONNECTION IN PLASMAS

J. B. Taylor

Culham Laboratory, Abingdon, Oxfordshire, OX14 3DB, England

(UKAEA/Euratom Fusion Association)

ABSTRACT

The theory of plasma relaxation is described and developed. Turbulence, allied with a small resistivity, allows the plasma rapid access to a particular minimum energy state. This process involves reconnection of magnetic field lines in a manner which destroys all the topological invariants of ideal plasma so that only total magnetic helicity survives. Although this mechanism, and the equations describing the relaxed state, are similar in all systems, the properties of the relaxed state depend crucially on the topology - toroidal or spherical - of the container and on the boundary conditions. Consequently, there are several different types of relaxed state each with its own special characteristics which are derived and discussed. The measurements made on many experiments, including Toroidal Pinches, OHTE, Multipinch, and Spheromaks are reviewed and shown to be in striking agreement with the theoretical predictions.

(Submitted for publication in Reviews of Modern Physics)

December 1985

CONTENTS

I. INTRODUCTION

A. Background

In this report a plasma is regarded as a conducting fluid having small resistivity and small viscosity. Even in this simple model interaction of the plasma with magnetic fields leads to extremely complex behaviour, especially when turbulence occurs. It is therefore remarkable that one can make quantitative predictions about the plasma configuration resulting from such turbulence. This is possible because the turbulence, allied with small resistivity, allows the plasma rapid access (in a time short compared with the usual resistive diffusion time) to a particular minimum energy state. This process, known as plasma relaxation, involves the reconnection of magnetic field lines and is a remarkable example of the self-organisation of a plasma (Hasegawa, 1985). Since plasma turbulence occurs frequently so do relaxed states, and the theory of relaxation has now been successfully applied to plasmas in many different laboratory systems (see references herein) and even to astro-physical plasmas (Heyvaerts and Priest, 1984; Konigl and Choudhuri, 1985).

An important concept in the theory is that of magnetic helicity, $\int \underset{\sim}{A} \cdot \underset{\sim}{B} d\tau$, as an invariant of plasma motion. This was used by Woltjer (1958) and by Wells and Norwood (1969) but relaxation theory as described here began with the work of Taylor (1974a, 1975, 1976) which explained why total helicity alone, rather than the infinity of invariants of ideal magnetohydrodynamics, should be important and determined the properties of the relaxed states of toroidal plasmas. These calculations showed that

the relaxed state accounted quantitatively for many hitherto unexplained observations on toroidal pinch experiments.

The toroidal pinch is one of the simplest systems for confining plasma by a magnetic field. In principle it involves only a toroidal vacuum vessel in which a toroidal magnetic field B_0 is first created by external coils (Fig. 1). Then, after creating an initial plasma by a suitable ionizing process, a toroidal current I is induced. This current heats and compresses the plasma through the well-known "pinch-effect". [For details of toroidal pinch experiments see, for example, the review by Bodin and Newton (1980).]

There are several remarkable features common to all toroidal pinch experiments. First, it is found that after an initial highly turbulent phase, the plasma settles into a more quiescent state in which the fluctuations are reduced. Second, in this quiescent state the mean magnetic field profiles are essentially independent of the particular experiment or the previous history of the discharge and depend only on a single parameter, the pinch ratio $\theta \equiv 2I/aB_0$. Third, if θ exceeds a certain critical value the quiescent state is one in which the toroidal field is spontaneously reversed in the outer region of the plasma near the vessel wall (hence the usual designation - Reversed Field Pinch, RFP). Typical mean magnetic field profiles are shown in Fig. 2.

It is clear from this behaviour of plasma in the toroidal pinch that during the turbulent phase it seeks out a preferred configuration - the relaxed state. The idea of a relaxed state can be illustrated by a simple analogy. Suppose a flexible, current carrying, closed-loop of wire is

immersed in a viscous medium; what configuration would it adopt when in equilibrium with its own magnetic field? So long as the wire is moving energy is dissipated, so it will come to rest in a state of minimum energy subject to whatever constraints are applicable. The magnetic constraint is that (LI) be constant (where L is the inductance) and the equilibrium, or relaxed state, is found by minimising $LI^2/2$ subject to this constraint. (This corresponds to a state of maximum inductance.)

B. Plasma Relaxation

A plasma resembles an infinity of interlinked flexible conductors and the problem is to identify the appropriate constraints. If there were no constraints the state of minimum energy would be a vacuum field with no plasma current. This is indeed the eventual state of an isolated resistive plasma but is clearly not what we are concerned with here. At the other extreme, if the plasma is perfectly conducting there is an infinity of constraints. These arise because the fluid moves precisely with the magnetic field, each field line maintains its identity and the flux through any closed curve moving with the fluid is constant.

To express these constraints mathematically (Taylor, 1974a) we introduce the vector potential, $\underset{\sim}{B} = \nabla \times \underset{\sim}{A}$, which satisfies

$$\frac{\partial \underset{\sim}{A}}{\partial t} = \underset{\sim}{v} \times \underset{\sim}{B} + \nabla\chi \quad . \tag{1.1}$$

Clearly, any variation of $\underset{\sim}{A}$ perpendicular to $\underset{\sim}{B}$ can be accommodated by

a suitable choice of $\underset{\sim}{v}$, so Eq. (1.1) imposes no constraint on $\delta\underset{\sim}{A}_\perp$. However, despite the arbitrary gauge χ, there are constraints on $\delta A_\parallel$, the variation parallel to $\underset{\sim}{B}$. From Eq. (1.1) we have

$$\underset{\sim}{B}\cdot\nabla\chi = \underset{\sim}{B}\cdot\frac{\partial\underset{\sim}{A}}{\partial t} \quad . \tag{1.2}$$

This is a magnetic differential equation (Kruskal and Kulsrud, 1958) for χ which can be satisfied only if

$$\oint \frac{d\ell}{B}\left(\underset{\sim}{B}\cdot\frac{\partial\underset{\sim}{A}}{\partial t}\right) \qquad \text{and} \qquad \oint \frac{dS}{|\nabla\psi|}\left(\underset{\sim}{B}\cdot\frac{\partial\underset{\sim}{A}}{\partial t}\right) \tag{1.3}$$

are zero on each closed field line and each magnetic surface respectively. The variation $\delta A_\parallel$ must be constrained accordingly. A convenient way to express this constraint (Taylor, 1974a) is: for every infinitesimal flux tube surrounding a closed line of force the quantity

$$K(\alpha,\beta) = \int_{\alpha,\beta} \underset{\sim}{A}\cdot\underset{\sim}{B}\, d\tau \tag{1.4}$$

is an invariant. (Here α,β label the line of force.) This infinity of invariants replaces the single invariant (LI) of the flexible wire loop. Note that these invariants are essentially <u>topological</u> - they involve the identification of lines of force and represent the linkage of lines of force with one another (Moffatt, 1978; Berger and Field, 1984). They state that if one closed field line initially links another n-times then in a perfectly conducting plasma the two loops must remain linked n-times during any plasma motion.

If we minimise the magnetic energy,

$$W = \frac{1}{2} \int (\nabla \times \underset{\sim}{A})^2 \, d\tau \tag{1.5}$$

subject to the infinity of constraints described above, then for a plasma confined by a perfectly conducting toroidal shell we find that the equilibrium state satisfies

$$\nabla \times \underset{\sim}{B} = \lambda (a,b) \underset{\sim}{B} \, . \tag{1.6}$$

Thus the state of minimum magnetic energy when all the constraints of a perfectly conducting plasma are observed is some force-free equilibrium. (This is hardly surprising since the plasma internal energy has been ignored.) However, this cannot be the appropriate description of the quiescent state, for in order to determine the Lagrange multiplier* $\lambda(a,b)$ one would have to calculate the invariant $K(\alpha,\beta)$ for each closed field line and relate it to its initial value. Hence, far from being universal and independent of initial conditions, the state defined by Eq. (1.6) depends on every detail of the initial state.

---

*Strictly, the minimisation cannot be treated by a simple Lagrange multiplier since the paths over which the constraints are applied themselves vary with $\delta\underset{\sim}{A}$. An extension of the technique is necessary but the final result is indeed the simple one of Eq. (1.6).

To escape from this dilemma we must recognise that real plasmas, especially turbulent ones, are never perfectly conducting in the sense discussed above. In the presence of resistivity, however small, topological properties of lines of force are no longer preserved. Lines of force may break and re-connect even though the resistive diffusion time may be very long and there is insignificant flux dissipation. Mathematically the situation is one of non-uniform convergence; when $\eta = 0$ the equations do not permit changes in the topology of field lines whereas such changes may occur when $\eta \neq 0$, even in the limit of small η. Physically, as $\eta \to 0$ the regions over which resistivity acts gets smaller but the field gradients get correspondingly larger and the rate of reconnection does not diminish as fast as η and may not diminish at all. Furthermore the effect of local reconnection is felt throughout the plasma. A similar process is involved in resistive instabilities (Furth et al., 1963; Furth, 1985) and magnetic reconnection at X-points (Sweet, 1958; Parker, 1957; Petschek, 1965). [See also reviews by Vasyliunas (1975), and White (1983).]

We conclude that in a turbulent resistive plasma, flux tubes have no continuous independent existence. Consequently all the topological invariants $K(\alpha,\beta)$ cease to be relevant, not because the magnetic flux changes significantly but because it is no longer possible to identify the field line to which the flux belongs. However, the sum of all the invariants, that is the integral of $\underset{\sim}{A} \cdot \underset{\sim}{B}$ over the total plasma volume V_0, is independent of any topological considerations and of the need to identiify field lines. Consequently it remains a good invariant so long as the resistivity is small. [For a discussion of another aspect of flux tubes in turbulent plasmas see Rusbridge (1977), (1982) and for a more

mathematical view of the uniqueness of the helicity invariant see Hameiri and Hammer (1982).]

To obtain the relaxed state of a slightly resistive turbulent plasma, therefore, we must minimise the energy subject to the single constraint that the <u>total</u> magnetic helicity

$$K_0 = \int_{V_0} \underset{\sim}{A} \cdot \underset{\sim}{B} \, d\tau \qquad (1.7)$$

be invariant. For a plasma enclosed by a perfectly conducting toroidal shell the corresponding equilibrium satisfies

$$\nabla \times \underset{\sim}{B} = \mu \underset{\sim}{B} \qquad (1.8)$$

where μ is a constant. This relaxed state depends only on a single parameter μ - which is directly related to the pinch parameter $\theta = \mu a/2$. (Already, therefore, this reproduces one aspect of the quiescent state.)

C. Boundary conditions and the invariant

Before discussing the nature of the relaxed states defined by Eq. (1.8) a comment is needed on the boundary conditions. At a perfectly conducting boundary the normal component B_n of the magnetic field is fixed. For the present we consider only $B_n = 0$ which is appropriate for the Toroidal Pinch and some other systems. One consequence of the perfectly conducting boundary is that the toroidal flux ψ in the plasma

is invariant. For the vector potential $\underset{\sim}{A}$ the boundary conditions in a toroidal system require that $\oint \underset{\sim}{A}\cdot d\underset{\sim}{\ell}$ and $\oint \underset{\sim}{A}\cdot d\underset{\sim}{s}$ (where $\oint d\underset{\sim}{\ell}$ and $\oint d\underset{\sim}{s}$ denote loop integrals along closed paths the long and short way around the toroidal boundary) should be fixed. In this case $\oint \underset{\sim}{A}\cdot d\underset{\sim}{s}$ prescribes the toroidal flux ψ .

Some features of the invariant K_0 should also be noted. One of these concerns gauge invariance. Under a gauge transformation $\underset{\sim}{A} \to \underset{\sim}{A} + \nabla\chi$ the change in the helicity K_0 is

$$\int \underset{\sim}{B}\cdot\nabla\chi \;=\; \oint \chi\, \underset{\sim}{B}\cdot d\underset{\sim}{S} \quad . \tag{1.9}$$

With the boundary condition $\underset{\sim}{B}\cdot\underset{\sim}{n} = 0$ the surface integral vanishes and K_0 is indeed gauge-invariant. Nevertheless, difficulties over gauge may arise because the interior of the torus is a multiply-connected region in which χ may not be single-valued. To overcome this it is sometimes convenient (Bevir and Gray, 1980; Taylor 1980) to replace K_0 by

$$K_1 \;=\; \int \underset{\sim}{A}\cdot\underset{\sim}{B} - \oint \underset{\sim}{A}\cdot d\underset{\sim}{\ell} \oint \underset{\sim}{A}\cdot d\underset{\sim}{s} \tag{1.10}$$

where $d\underset{\sim}{\ell}$ and $d\underset{\sim}{s}$ again denote loop integrals the long and short way around the toroidal surface. If a complete conducting shell surrounds the plasma these loop integrals are constant and nothing in our discussion is changed; K_1 is invariant during relaxation just as K_0 is. The advantage of (1.10) is that it is manifestly gauge-invariant even for multivalued gauge potentials.

If the boundary of the plasma is not a flux surface (i.e. $B_n \neq 0$

everywhere on the boundary) then (1.9) is non-zero and the helicity is not well-defined. This reflects the fact that $\underset{\sim}{A}\cdot\underset{\sim}{B}$ is not a local quantity. One cannot specify the 'local' helicity at a point - only the total helicity within a flux surface. Where the helicity is located within that surface is not a valid question, any more than is the related question of where the linkage between two interlinked hoops is located. Consequently the question of gauge invariance and the definition of helicity must be reconsidered when we discuss systems in which $(B_n) \neq 0$ on the boundary (Section VIB).

Although total helicity K is invariant when the plasma is enclosed within a complete conducting shell, it does change when an external loop voltage V_ℓ is applied across a gap in the toroidal shell (as when the discharge is first created). According to (1.10) this change can be expressed as

$$\frac{dK_1}{dt} = 2V_\ell\psi \qquad (1.11)$$

where ψ is the toroidal flux. This shows that helicity can be given a practical interpretation (Taylor, 1975); at constant toroidal flux it is proportional to the Volt-seconds stored in the discharge. Equation (1.11) also shows that by suitably phased simultaneous oscillation of V_ℓ and ψ, helicity can be continuously fed into the plasma without the need for a continuous supply of Volt-seconds (Bevir and Gray, 1980). The mean rate of helicity injection is

$$\left\langle\frac{dK_0}{dt}\right\rangle = \left\langle\frac{dK_1}{dt}\right\rangle = 2\langle\tilde{\tilde{V}}\tilde{\psi}\rangle \ . \qquad (1.12)$$

D. Plasma Pressure

A comment is also necessary on the role of plasma pressure. Relaxation proceeds by reconnection of lines of force and during this reconnection plasma pressure can equalise itself so that the fully relaxed state is also a state of uniform pressure. Hence the inclusion of plasma pressure does not change our conclusions about the relaxed state. Of course, one may argue that pressure relaxation might be slower than field relaxation so that the former was incomplete and some pressure gradients would remain. A pressure gradient can be introduced directly (Edenstrasse and Schuurman, 1983; Kondoh, 1981) or by incorporating additional invariants (Bhattacharjee et al., 1980; Bhattacharjee and Dewar, 1982; Turner and Christiansen, 1981). However, no convincing argument for determining the correct residual pressure gradient has yet been given. We shall, therefore, consider ∇p to be negligible in relaxed states - which in any event is a good approximation for low-β plasmas.

II. RELAXED STATE IN LARGE ASPECT RATIO TORUS

We now return to the properties of the relaxed state defined by Eq. (1.8). For a circular cross-section torus of large aspect ratio we may take the cylindrical limit in which the solution to Eq. (1.8) is

$$B_r = 0 \quad , \quad B_\theta = \alpha J_1(\mu r) \quad , \quad B_z = \alpha J_0(\mu r) \quad . \tag{2.1}$$

This is the well-known "Bessel function" solution. By straightforward calculation μa (where a is the minor radius of the discharge) can be expressed as a function of K/ϕ^2 (Taylor, 1974a). Hence the field profiles in the relaxed state are determined by this ratio - though, as has been noted, it is usual to label the relaxed states by the pinch ratio θ ($= \mu a/2$) . Note that the relaxed state is completely determined by the two invariants K and ϕ ; the ratio K/ϕ^2 fixes the field profile and either K or ϕ then fixes the magnitude of the fields. No arbitrary or adjusted parameters are required in the theory.

The field profiles given by (2.1) agree well with those observed in the quiescent phase of many toroidal discharges. Figure 2 shows a comparison with measurements on HBTX-1A (Bodin, 1984). Many other toroidal pinch experiments show similar profiles. [Several such experiments are shown in Table I. For greater detail see the references cited.]

The onset of the spontaneous reversed toroidal field at the wall can also now be determined. It occurs when $\mu a > 2.4$, i.e. when the pinch ratio $\theta > 1.2$. This result too is in good agreement with many observations. The relevant experimental data is usually presented through an F-θ diagram, where F is the ratio of toroidal field at the wall to the average toroidal field ($F < 0$ implies reversal). Figure 3 shows points on the F-θ curve for several experiments (Bodin and Newton, 1980), together with the corresponding theoretical curve.

It is noteworthy that the experimental points in Fig. 3 do indeed all lie on a universal F-θ curve close to the theoretical one, although the

experimental value of θ for field reversal is somewhat higher than the theoretical value. One reason for this is that $\mu \equiv (\underset{\sim}{j} \cdot \underset{\sim}{B})/B^2$, which would be uniform in a fully relaxed state, in fact falls off near the wall. The observed profile of $\mu(r)$ in the OHTE experiment (Tamano et al., 1983; Ohkawa et al., 1980) is shown in Fig. 4. Similar profiles have been observed in the ETA-BETA (Antoni et al., 1983) and HBTX experiments (Bodin, 1984) and the effect of the $\mu(r)$ profile on the value of θ has been discussed in detail by Ortolani (1984). The fall in μ near the wall is believed to be due to the high plasma resistivity there -which the relaxation process cannot fully overcome.

Another reason for the discrepancy between the theoretical and experimental values of θ is that the measurements are often distorted by the flux conserving liner and by toroidal plasma shifts. In recent experiments where θ is corrected for these effects, the agreement between theory and experiment is further improved (Newton, 1985).

Even more striking evidence for relaxation is shown in the time dependent behaviour of toroidal pinches. This is illustrated in the time dependent F-θ curves in Figs. 5-6. Figure 5(a) (Bodin and Newton, 1980) shows that during a fast current rise in HBTX the discharge is temporarily forced away from the relaxed state, but quickly falls back to it and subsequently follows closely the theoretical F-θ curve. When the current rise is slower the discharge lies close to the theoretical curve throughout [Fig. 5(b)]. Similar F-θ curves for ZT-40 (DiMarco, 1983), for OHTE (Tamaru et al., 1978) and for REPUTE (Toyama et al., 1985) are shown in Fig. 6.

These results, and many others from the experiments listed in Table I, show that the theory presented here accounts extremely well for the features of toroidal discharges described in the introduction. We now turn to some additional consequences of the theory.

III. FURTHER PROPERTIES OF RELAXED STATES IN LARGE ASPECT RATIO TORUS

Determination of the relaxed state is actually more complex than we have indicated so far. This is because Eq. (1.8) may have several solutions compatible with the boundary conditions and with the given values of K and ψ. In this event, one must select that solution which has the lowest energy. The procedure can be demonstrated by considering again the large aspect ratio circular plasma (Taylor, 1975).

The general solution of Eq. (1.8) can be written (Chandrasekhar and Kendall, 1957) as

$$\underset{\sim}{B} = \sum a_{mk} \underset{\sim}{B}^{mk}(\underset{\sim}{r}) \qquad (3.1)$$

where the a_{mk} are arbitrary and the individual $\underset{\sim}{B}^{mk}$ are

$$B_r^{mk} = \frac{-1}{(\mu^2 - k^2)^{1/2}} \left\{ kJ_m'(y) + \frac{m\mu}{y} J_m(y) \right\} \sin(m\theta + kz)$$

$$B_\theta^{mk} = \frac{-1}{(\mu^2 - k^2)^{1/2}} \left\{ \mu J_m'(y) + \frac{mk}{y} J_m(y) \right\} \cos(m\theta + kz) \qquad (3.2)$$

$$B_z^{mk} = J_m(y) \cos(m\theta + kz)$$

with $y = r(\mu^2 - k^2)^{1/2}$.

Although this solution satisfies Eq. (1.8) we have not yet imposed the boundary condition $B_r(r=a) = 0$, nor have we considered the value of the invariant K or the toroidal flux ϕ . Before doing so an important feature of the above expressions should be noted. The $m = 0$, $k = 0$ term is different in character from all the others. It satisfies the boundary condition for any value of μ and carries a non-zero toroidal flux. All the other terms satisfy the boundary condition <u>only</u> for discrete values of μ given by

$$ka\left[(\mu^2 - k^2)^{1/2}a\right] J_m'\left[(\mu^2 - k^2)^{1/2}a\right] + m\mu a\, J_m\left[(\mu^2 - k^2)^{1/2}a\right] = 0 \ , \qquad (3.3)$$

and do not contribute any toroidal flux.

There are thus two distinct types of solution to Eq. (1.8) which could be made to satisfy the boundary conditions and correspond to the given toroidal flux. They are

1. The 'symmetric' $m = 0$, $k = 0$ solution which exists for any μ . For such a solution, as already noted, the appropriate value of μ is determined by the value of K/ψ^2 .

2. A 'mixed' solution containing the $m = 0$, $k = 0$ term (to give the required toroidal flux) together with one of the other terms, i.e. a solution $[\alpha_0 \underset{\sim}{B}^{00} + \alpha_{mk} \underset{\sim}{B}^{mk}]$. This mixed solution exists only for fixed discrete values of μ and the role of the invariant K/ψ^2 is no longer to determine μ . Instead K/ψ^2 determines the ratio α_{mk}/α_0.

We see that both types of solutions are completely defined by the two invariants K and ψ , but in a different way in the two cases. We now need to determine which solution has the lowest energy. (Note there is only one solution of type I but there are many of type II.) It can be shown that the lowest energy solution of Eq. (1.8) is that with the smallest μ (see Appendix, Section IXB), so of all possible solutions of the second type only that corresponding to the smallest root of Eq. (3.3) can be of interest. This smallest root occurs for $m = 1$, $ka \simeq 1.25$ and is given by $\mu a = 3.11$ (Martin and Taylor, 1974). See also Gibson and Whiteman (1968).

The selection of the appropriate solution can now be made. The first 'symmetric' solution is the lowest energy state for all values of K/ψ^2 which correspond to $\mu a < 3.11$. For any larger value of K/ψ^2 the lowest energy state is a 'mixed' solution with $\mu a = 3.11$ ($\theta \sim 1.6$) containing a helical component with $m = 1$ and $ka \simeq 1.25$. Since, for

fixed toroidal flux, K/ϕ^2 is proportional to Volt-seconds in the discharge the helical relaxed state arises when the Volt-seconds exceed a critical value. Furthermore, once that critical value is reached further Volt-seconds do not increase θ (or the plasma current at fixed toroidal flux) in the relaxed state. Instead the current channel becomes more helical and the increased inductive voltage absorbs the additional Volt-seconds.

Thus we see that the theory of relaxed states predicts not one, but two, critical values of θ for the toroidal discharge (Taylor, 1975). At $\theta = 1.2$ a reversed field is first generated and at $\theta = 1.6$ current saturation sets in. Evidence for this second critical θ was first found in HBTX1A (Bodin and Newton, 1980; Verhage et al., 1978; Butt et al., 1975) and is illustrated in Fig. 7. This shows a discharge in which θ was temporarily driven to a large value but quickly dropped back to around 1.6, where it remained for the rest of the discharge. The drop in θ was accompanied by the appearance of an $m = 1$ helical distortion.

Not all toroidal pinches show this current limitation, though there are usually increased fluctuations and a higher plasma resistance if θ is driven beyond a threshold at ~ 1.6. An example of this is shown in Fig. 8 (Watt and Nebel, 1983).

We shall later describe much clearer evidence for current limitation (Section V). First, however, we must say something more about relaxed states in general toroidal systems.

IV. GENERAL TOROIDAL RELAXED STATES

The general theory of toroidal relaxed states follows closely that for the large aspect ratio circular pinch (Jensen and Chu, 1984; Faber et al., 1982, 1985) and is described in the Appendix, Section IX. The present section is a summary of those features which are needed for the discussion of the Multipinch experiment and is restricted to axisymmetric systems.

In general the relaxed state of a toroidal system is the lowest energy solution of

$$\nabla \times \nabla \times \underset{\sim}{A} = \mu \nabla \times \underset{\sim}{A} \tag{4.1}$$

with $\underset{\sim}{n} \cdot \nabla \times \underset{\sim}{A} = 0$ on the boundary and with $\oint \underset{\sim}{A} \cdot d\underset{\sim}{s}$, $\oint \underset{\sim}{A} \cdot d\underset{\sim}{\ell}$ and the helicity K given. In order to describe the relevant solutions we need also to consider the associated eigenvalue problem

$$\nabla \times \nabla \times \underset{\sim i}{a} = \lambda_i \nabla \times \underset{\sim i}{a} \tag{4.2}$$

with boundary condition $\underset{\sim i}{a} = 0$. (Note that because of this boundary condition an eigenfunction carries no toroidal flux.)

As in the circular case, there can be many solutions of Eq. (4.1) which satisfy the boundary conditions and have the correct values of the invariants K and ψ $(= \oint \underset{\sim}{A} \cdot d\underset{\sim}{s})$ but only two of them are possible lowest-energy solutions. The first is an axisymmetric solution, analogous to the $m = 0$, $k = 0$ solution in the circular discharge. This may

exist for any value of μ except $\mu = \lambda_i$ and μ is determined by K/ψ^2. The second is a superposition of the first solution and the lowest eigenfunction (i.e. the eigenfunction with smallest positive* eigenvalue λ_0). In this mixed solution, $\mu = \lambda_0$ and K/ψ^2 determines the amplitude of the eigenfunction component.

Bearing in mind that the lowest energy solution is that with the smallest μ it is clear that the first solution describes the relaxed state when K/ψ^2 is small and the corresponding μ is less than λ_0. The second solution describes the relaxed state for larger K/ψ^2, when $\mu > \lambda_0$ in the first solution. In this event the toroidal current (at fixed toroidal flux) is fixed and does not increase with K/ψ^2. [Strictly, this second solution arises only if the lowest eigenfunction is 'decoupled', in the sense defined in the Appendix, but this is usually the case in axisymmetric systems. If the lowest eigenfunction is not decoupled only the first type of solution is relevant. However, in this event $K/\psi^2 \to \infty$ as $\mu \to \lambda_0$ so that it is still true that μ can never exceed the smallest eigenvalue and that current saturation occurs at this point.]

Although the relaxed states of general axisymmetric systems are similar to those in the large aspect circular system, there is one important feature of the general system which is not apparent in the circular example. In that example the lowest eigenvalue ($\mu a = 3.11$) corresponds to a non-axisymmetric eigenfunction, in fact to a helical mode with $m = 1$, $ka = 1.25$. [The lowest axisymmetric ($k = 0$) eigenvalue

---

*For systems with minor symmetry the eigenvalues occur in pairs $\pm \lambda_i$.

is $\mu a = 3.83$ and is degenerate.] For many other cross-sections the lowest eigenfunction is also non-axisymmetric, but in a highly convoluted cross-section the lowest eigenfunction may be axisymmetric. This is the case for the configuration of the 'Multipinch' experiment discussed in the next section and, as we shall see, it has important consequences.

V. THE MULTIPINCH EXPERIMENT AND AXISYMMETRIC RELAXED STATES

The Multipinch, investigated at GA Technologies (La Haye et al., 1984; La Haye et al., 1985), is an example of an axisymmetric toroidal system with non-circular cross-section. The cross-section resembles a figure-8 whose height is about 2.5 times its width (Fig. 9). The major radius is 52.5 cm, the height 50 cm and the width 20 cm. The dimensions were chosen so that the Multipinch is roughly equivalent to two circular cross-section pinches [actually TPE-1R(M)] one above the other. The method of operation is similar to other toroidal pinch experiment.

Axisymmetric relaxed states of the Multipinch are readily found. An axisymmetric field can be written, in cylindrical coordinates R, ϕ, Z as:

$$\underset{\sim}{B} = \frac{\underset{\sim}{e}_\phi \times \nabla\chi}{R} + \frac{\underset{\sim}{e}_\phi f}{R} \quad . \tag{5.1}$$

Then for the relaxed state, Eq. (4.1) gives

$$\Delta^+\chi \equiv \frac{\partial^2\chi}{\partial Z^2} + R\,\frac{\partial}{\partial R}\left(\frac{1}{R}\,\frac{\partial\chi}{\partial R}\right) = \mu f \tag{5.2}$$

and

$$\nabla f = -\mu \nabla \chi \qquad (5.3)$$

so that $f = C - \mu\chi$. The boundary condition is χ = constant and without loss of generality this constant can be set to zero. The toroidal flux condition then gives

$$\Psi = -\mu \int \frac{\chi}{R}\, dRdZ + C \int \frac{1}{R}\, dRdZ \qquad (5.4)$$

so defining a toroidally weighted average,

$$\langle \bullet \rangle \equiv \left[\int \bullet \frac{1}{R}\, dRdZ\right]\left[\int \frac{1}{R}\, dRdZ\right]^{-1} , \qquad (5.5)$$

the equation for axisymmetric relaxed states becomes (La Haye et al., 1985):

$$\Delta^{+}\chi + \mu^2\chi - \mu^2\langle\chi\rangle = \frac{\mu\langle R\rangle\Psi}{A} \qquad (5.6)$$

where A is the cross-section area of the discharge.

The corresponding axisymmetric eigenvalue problem, Eq. (4.2), becomes

$$\Delta^{+}\chi_i + \lambda_i^2 \left(\chi_i - \langle\chi_i\rangle\right) = 0 \qquad (5.7)$$

with $\chi_i = 0$ on the boundary.

Solutions of Eq. (5.6) can easily be computed, and an example of the relaxed state at $\mu a = 1.5$ is shown in Fig. 10 (La Haye et al., 1985; Taylor and Turner, 1985). This configuration is symmetric in the upper and lower halves of the cross-section and B_ϕ is everywhere of the same sign.

Similarly the eigenfunctions, Eq. (5.7), can also be computed. The lowest eigenvalue is found to be $\mu a = 2.21$ (La Haye et al., 1985). The corresponding eigenfunction, shown in Fig. 11, is antisymmetric in the two halves of the cross-section, i.e. B_ϕ is of opposite sign in the upper and lower halves.

The axisymmetric relaxed states can also be described in terms of the toroidal field. The function f satisfies

$$\Delta^* f + \mu^2 f = 0 \qquad (5.8)$$

with f constant around the boundary. In this description there is no direct reference to the toroidal flux Ψ, which must be introduced through the requirement that

$$\langle f \rangle = \frac{\langle R \rangle \Psi}{A} \, . \qquad (5.9)$$

The associated eigenvalue problem is also described by (5.8) with f constant on the boundary so there may appear to be no eigenvalue condition. In fact this arises separately from the vanishing-flux condition

$$\langle f \rangle = 0 \quad . \tag{5.10}$$

One now sees that it is important to distinguish between this eigenvalue problem (problem A) and the simpler eigenvalue problem defined by (5.8) with f = zero on the boundary (problem B). Problem A is entirely equivalent to Eq. (5.7) for χ_i with $\chi_i = 0$ on the boundary and its lowest eigenvalue determines the point of current saturation. An eigenvalue of problem B, on the other hand, can at most determine a point at which the toroidal field vanishes at the wall, i.e. a point of 'field-reversal' $F = 0$.

The two eigenvalue problems are quite distinct. However, when there is an equatorial plane of symmetry, some of the eigenfunctions χ_i for problem A are antisymmetric about this plane. For such eigenfunctions $\langle \chi_i \rangle = 0$ so Eq. (5.7) and its boundary condition are then identical with Eq. (5.8) and its boundary condition in problem B. Consequently the two problems then have a common solution and a common eigenvalue.

This coincidence occurs in the Multipinch, where the lowest eigenvalue ($\mu a = 2.41$) of problem A (determining current saturation) coincides with the second-lowest eigenvalue of problem B. Furthermore, this second eigenvalue of problem B is very close to the first, which determines field reversal. [The first and second eigenvalues of problem B differ by only $\sim 2\%$ (Taylor and Turner, 1985): they would be exactly degenerate if the gap between the two lobes of the figure-eight were infinitesimal.] As a result, field reversal and current saturation are almost coincident in the Multipinch.

In the Multipinch, therefore, the relaxed state for small values of K/ψ^2 (low Volt-seconds) is axisymmetric and symmetric about the equatorial plane. In this relaxed state μa and the plasma current increase with Volt-seconds. However when μa reaches 2.21 the relaxed state changes to one which is no longer symmetric about the equatorial plane (i.e. more current flows in one lobe of the figure-8 than the other), although it remains axisymmetric. The 'up-down' asymmetry increases with increasing Volt-seconds but μa and the total current are fixed and $F = B_\phi(\text{wall})/\langle B_\phi \rangle$ is almost zero.

These features of the relaxed state are all clearly demonstrated in the Multipinch experiment. Figure 12 (La Haye et al., 1985) shows the peak plasma current I_p (at fixed toroidal flux $\langle B_z \rangle$) as a function of the capacitor-bank voltage V_{CB} [the voltage applied to the primary circuit of which the plasma forms the secondary; K/ψ^2 increases roughly linearly with V_{CB}]. At low voltage the configuration is axisymmetric and symmetric about the equatorial plane and the current increases with V_{CB}. At higher V_{CB} the current saturates and the discharge acquires an 'up-down' asymmetry which increases with further increase in V_{CB}. The current saturation and the onset of 'up-down' asymmetry almost coincide with vanishing toroidal field at the wall, i.e. with $F = 0$.

It can also be seen from Fig. 12 that the saturation current depends on $\langle B_z \rangle$, i.e. on the toroidal flux Ψ. The variation of saturation current with toroidal flux is shown in Fig. 13. The straight line corresponds to $\mu a = 2.42$ and is thus in very good agreement with the theoretical value (2.21).

One may ask why current saturation is more clearly demonstrated in the Multipinch than in the circular cross-section pinch. This is probably because in the circular pinch the current saturated state is reached only after toroidal field reversal and so involves reverse current flow near the wall and strong plasma-wall interaction. (See also Mannheimer (1981).) Such currents are inhibited by the low plasma conductivity in this region. On the other hand, because of the coincidence between toroidal field reversal and current saturation, no such reverse current is called for in the Multipinch.

In theory, the up-down asymmetry of the Multipinch in the current saturated state should increase indefinitely with increasing voltage, until eventually the current in one half of the cross-section would be reversed. In practice the asymmetry increases until the current in one half falls to zero and the discharge is entirely confined to the other half. From that point on it acts as a circular cross-section discharge confined to one half of the machine - with the other half acting somewhat as an external inductance.

VI. RELAXED STATES IN OTHER SYSTEMS

A. Spheromak

So far we have considered relaxation only for toroidal systems. However, relaxed states are of equal importance in another class of plasma configurations of which the prototype is the Spheromak, Fig. 14. In this configuration (Rosenbluth and Bussac, 1979), the magnetic field has nested toroidal surfaces as in a toroidal pinch, but the confining shell is topologically spherical instead of toroidal. Of course, although the spherical topology is essential the actual shape need not be a true sphere.

The distinguishing feature of a Spheromak is that there is no central aperture for toroidal field coils: consequently the toroidal field is everywhere zero at the wall and in this respect the spheromak resembles a toroidal pinch at the point of field reversal, with $F = 0$. However, in the pinch the vanishing toroidal field implies that $q(\psi) = 2\pi/\iota(\psi)$ (where $\iota(\psi)$ is the rotational transform of lines of force on the surface ψ) is zero at the wall, whereas in the Spheromak this is not the case. The factor $q(\psi)$ represents an average over the flux surface and although the toroidal field tends to zero over part of the surface $q(\psi)$ remains finite. In fact, for a truly spherical system $q(\psi)$ decreases only from 0.825 on the magnetic axis to 0.72 at the wall (Rosenbluth and Bussac, 1979).

Plasma formation in the Spheromak is considerably more difficult to visualise than it is in the toroidal pinch (Goldenbaum, 1982; Furth, 1981). In one method, used in the CTX, Beta II and CTCC-1 experiments (Jarboe et al., 1980, 1983; Turner et al., 1981, 1983; Nagata et al., 1984), a plasma is produced by a coaxial plasma-gun and injected into a confinement chamber (Fig. 15). Plasma formed in the gun carries both poloidal field, provided by coils in the gun, and toroidal field produced by plasma currents. The magnetic forces eject the plasma from the gun into the container (known as the flux-conserver) where it relaxes into a Spheromak configuration. Another method for forming a Spheromak plasma employs a combination of θ- and z-pinch discharges, as in the PS-1 and TODAI experiments (Goldenbaum et al., 1980; Nogi et al., 1980; Bruhns et al., 1983; Katsurai et al., 1984). This process is illustrated in Fig. 16.

Spheromak plasmas can also be formed by a slow inductive process as in the S-1 experiment (Fig. 17) (Yamada et al., 1981). An initial poloidal field is generated by current in a ring-shaped (toroidal) flux core, and is weakened on the small-major-radius side of the core by an externally generated vertical field. The flux-core also contains a toroidal solenoid, which generates a toroidal flux within it. When this toroidal solenoid is energized it induces poloidal current in plasma surrounding the ring. The associated toroidal field distends the plasma, stretching it towards the axis. Then the toroidal current in the flux-core is reversed and additional toroidal current induced in the plasma. Reconnection of the poloidal field occurs and a separated plasma toroid is created on the small-major-radius side of the flux core. This toroid, the desired Spheromak configuration, is held in equilibrium by the external vertical field.

The parameters of several Spheromak experiments are shown in Table II. The references cited should be consulted for more details.

1. Relaxed states of Spheromak

As in the toroidal systems, the helicity $K_0 = \int \underset{\sim}{A} \cdot \underset{\sim}{B} d\tau$ is conserved during relaxation in the Spheromak and the relaxed state satisfies

$$\nabla \times \nabla \times \underset{\sim}{A} = \mu \nabla \times \underset{\sim}{A} \quad . \tag{6.1}$$

Despite this formal similarity, however, there is a significant difference between the theory of relaxed states in the Spheromak and in the toroidal pinch. In a toroidal device one has two invariant quantities, the helicity K and the toroidal flux ϕ, and, as we have seen, these are just sufficient to determine the relaxed state. In the Spheromak, toroidal flux ϕ is not a conserved quantity; annihilation and creation of flux can occur at the axis of symmetry. Consequently one has only a single invariant K from which to determine the relaxed state.

On the other hand, the Spheromak is a singly-connected volume and $\oint \underset{\sim}{A} \cdot d\underset{\sim}{s}$ vanishes over <u>any</u> closed path in the bounding surface. Apart from a gauge transformation this is equivalent to setting $\underset{\sim}{A} = 0$ on the boundary so that the only possible solutions of (6.1) for a Spheromak are eigenfunctions and the only possible values for μ are the corresponding eigenvalues.

It is therefore much simpler to find the relaxed state in a Spheromak than in a toroidal pinch! There is no need to select from different types of solution, the relaxed state is just the eigenfunction corresponding to the smallest eigenvalue of Eq. (6.1). The value of μ and the field profiles are thus determined by the shape of the container alone. The role of the single invariant K is only to fix the magnitude of the magnetic field and the toroidal flux ϕ plays no direct role in determining the relaxed state.

The axisymmetric eigenfunctions for Spheromak-like systems are easily found. The magnetic field is again expressed in the form (5.1) and the eigenvalue problem for a Spheromak reduces to

$$\Delta^{+}\chi_i + \mu_i^2\chi_i = 0 \qquad (6.2)$$

with $\chi_i = 0$ on the boundary. For simple containers the eigenfunctions can be obtained analytically and for more complex shapes they are readily computed.

In a spherical container of radius a the lowest eigenvalue is given by $\mu a = 4.49$ and the corresponding eigenfunction is

$$B_r = 2B_0\left(j_1(\mu\rho)/\mu\rho\right)\cos\theta$$

$$B_\phi = B_0\, j_i(\mu\rho)\,\sin\theta \qquad (6.3)$$

$$B_\theta = -B_0\,\frac{d}{d\rho}\left[\rho j_1(\mu\rho)\right]\sin\theta$$

where ρ , θ , ϕ are spherical coordinates and $j_1(x) = J_{3/2}(x)/x^{1/2}$ (Rosenbluth and Bussac, 1979).

In a cylindrical container of height h and radius a the lowest eigenvalue is

$$\mu = \left[\left(\frac{3.83}{a}\right)^2 + \left(\frac{\pi}{h}\right)^2\right]^{1/2} \qquad (6.4)$$

(for h/a less than a critical value, see below) and the corresponding eigenfunction is

$$B_r = -B_0 k\, J_1(\ell r)\cos(kz)$$

$$B_\phi = B_0\mu\, J_1(\ell r)\sin(kz) \qquad (6.5)$$

$$B_z = B_0 k\, J_0(\ell r)\sin(kz)$$

where $kh = \pi$, $\ell a = 3.83$ and r, ϕ, z are cylindrical coordinates (Finn et al., 1981; Bondeson et al., 1981).

The eigenfunctions (6.3) and (6.5) are axisymmetric, but it is also possible for the lowest eigenvalue to be that of a non-axisymmetric mode. Whether this is so depends on the shape of the container. For example, in a cylindrical container, the axisymmetric eigenfunction described above has the lowest eigenvalue only when $h/a \lesssim 1.67$. When $h/a > 1.67$ there is a non-axisymmetric mode with a lower eigenvalue and in this case the relaxed state is non-axisymmetric (Finn et al., 1981; Bondeson et al., 1981).

2. Spheromak experiments

Measurements have been made of relaxed state plasmas in several Spheromak experiments. Some of the data from the Beta-II experiment (which has a roughly cylindrical flux conserver with $h/a \simeq 1$) is illustrated in Fig. 18 (Turner et al., 1983). This shows the measured poloidal and toroidal fields together with the theoretical profiles for the relaxed state given by Eq. (6.5). The agreement is very satisfactory, particularly in view of the complex way in which the plasma is formed. It should also be noted that the field profiles retained their theoretical form as the energy in the discharge decayed to about one-eighth of its initial value. Furthermore, except for a cut-off when the Volt-seconds are too low or the magnetic flux in the gun too high, the magnetic flux in the initial relaxed state was proportional to the square root of the helicity produced by the gun - as required by the theory.

Confirmation that μ ($\equiv \underset{\sim}{j}\cdot\underset{\sim}{B}/B^2$) is uniform in the relaxed state of a Spheromak is provided by Fig. 19 (Hart et al., 1985). This shows the

poloidal current vs. poloidal flux in the S-1 experiment (which has an ellipsoidal plasma). Not only do the observations lie on a straight line, corresponding to uniform μ, but the slope of the line also agrees well with the calculated value of μa. A more detailed picture of μ is given in Fig. 20 which shows the profile before and after relaxation, as well as the theoretical value.

The most striking feature of S-1, however, occurs during relaxation itself (Janos et al., 1985). Figure 21 shows the evolution of the poloidal and toroidal fluxes and of q on the magnetic axis during the relaxation phase. This indicates that during relaxation q rises rapidly from its initial very small value to its theoretical predicted value (0.65 for the ellipsoidal configuration of the S-1 plasma). This development is accompanied by destruction of poloidal flux and the spontaneous creation of toroidal flux in a very short time compared with the resistive decay time. Furthermore, following relaxation, q remains constant during the resistive decay of the plasma, demonstrating the persistence of the relaxed configuration.

B Flux Core Spheromak (FCS)

An interesting development of the Spheromak is a configuration obtained from it by introducing a central core of externally produced magnetic flux along the axis of symmetry (Fig. 22). This externally linked flux enters through one polar cap and leaves through the other. [Of course the actual boundary may again depart significantly from the spherical form. See Jensen and Chu (1981), (1983).] Although the FCS has

toroidal flux surfaces and may appear to resemble a Toroidal Pinch, it is in fact completely different. Unlike the Toroidal Pinch there is only plasma in the central core, not a fixed conductor; consequently toroidal flux is not a conserved quantity.

1. Relative helicity

In the FCS configuration the plasma container is <u>not</u> a flux surface and we have already noted that in this event the helicity K is not well defined. Some change in the definition of helicity is therefore needed to deal with the Flux-Core Spheromak and similar systems.

One method (Berger and Field, 1984) is to imagine that the flux leaving and entering the boundary is extended outside as a vacuum field ($\nabla \times \underset{\sim}{B} = 0$) . Then the total helicity $\int \underset{\sim}{A} \cdot \underset{\sim}{B}$ inside and outside the sphere <u>is</u> a well defined quantity. Furthermore, if the bounding surface of the sphere is perfectly conducting the normal component of $\underset{\sim}{B}$ is "frozen in" so that changes in the interior field do not affect the hypothetical field outside. We may then consider the difference in helicity of two fields which differ inside the Spheromak but have identical normal field components on the boundary and hence identical hypothetical extension fields outside. This difference, the relative helicity of the two configurations, is well-defined and gauge invariant. [Note that it is necessary to include the contribution to $\int \underset{\sim}{A} \cdot \underset{\sim}{B}$ from both the interior and exterior regions even though the exterior field does not

change. This reflects the fact that helicity is not a local quantity and can be transferred, within a flux surface, from the interior to the exterior of the container by a gauge transformation!]

Of course, to make use of the relative helicity K_R we must show that it is invariant during relaxation. A straightforward calculation gives

$$\frac{dK_R}{dt} = 2\int_{\text{interior}} \underset{\sim}{E}\cdot\underset{\sim}{B}\, d\tau + 2\int_{\text{exterior}} \underset{\sim}{E}\cdot\underset{\sim}{B}\, d\tau \quad . \tag{6.6}$$

The hypothetical exterior magnetic field is constant during relaxation, so $\nabla \times \underset{\sim}{E} = 0$. Thus $\underset{\sim}{E} = \nabla\phi$, where ϕ is a single valued function and

$$\frac{dK_R}{dt} = 2\int_{\text{interior}} \underset{\sim}{E}\cdot\underset{\sim}{B} + 2\oint \phi\underset{\sim}{B}\cdot d\underset{\sim}{S} \quad . \tag{6.7}$$

When the bounding surface is equipotential, ϕ is constant over it and the surface integral vanishes. The interior integral is the usual one for any system and is negligible on the relaxation time scale for a highly conducting plasma ($E_{\|} \sim 0$) . Consequently K_R is indeed invariant during relaxation.

Equation (6.7) also shows that helicity may be injected or extracted from the FCS if one of the polar caps is electrically insulated and maintained at a different potential to the other. Then helicity is changed at a rate (Taylor, 1975, 1976; Jensen and Chu, 1984)

$$\frac{dK_R}{dt} = 2V_p\psi_p \qquad (6.8)$$

where V_p is the voltage between the polar caps and ψ_p is the flux through them. This provides another method of sustaining a relaxed state against resistive decay. [It also describes the production of helicity in plasma guns (Turner et al., 1983).]

2. Relaxed states

The relaxed state of a Flux Core system is obtained by minimising the energy subject to K_R being invariant and with the boundary condition that the normal component of $\underset{\sim}{B}$ be constant . Once again this leads to the equation for relaxed states

$$\nabla \times \underset{\sim}{B} = \mu \underset{\sim}{B} \qquad (6.9)$$

but for the new system there are new interpretations! Before discussing these we should remark that by neglecting all other constraints of the type $K(\alpha,\beta)$ = constant we are implying that in the Flux Core Spheromak turbulence can produce linking between flux lines which thread the polar caps and those which do not, i.e. the separatrix between the externally linked flux and the internal flux is not preserved during turbulence.

For a Flux Core System, the interpretation of Eq. (6.9) which most closely resembles its interpretation for toroidal systems (Section III) is applicable when the plasma relaxes from an initial state with given

helicity K_R and with given flux ψ_p through the polar caps. Then the value of μ is determined by the ratio K_R/ψ_p^2 (in rather the same way that the symmetric state of a toroidal pinch is determined by K/ψ^2) and the magnitude of the field is determined by ψ_p, so that the relaxed state is fully determined by the two invariants K and ψ_p. This interpretation describes the situation immediately following relaxation. It assumes that the polar caps can supply whatever current is required in the relaxed state; if they cannot do so the resulting voltage drop would reduce the helicity until the relaxed state corresponded to the current available.

The fact that voltages on the polar caps can change the helicity leads to a second interpretation of Eq. (6.9) for FCS systems. If one of the polar caps, say that in which $B_n > 0$, is electrically insulated from the rest of the container (e.g. by a thin annular gap) and connected to a suitable circuit, then μ can be controlled by the current I_p through it; $\mu = I_p/\psi_p$. (The magnitude of the field is still determined by the polar-cap flux ψ_p.) This view of Eq. (6.9) describes a steady state FCS in which initial conditions are no longer significant. The helicity K_R is not then independently specified but reaches the value required to conform with μ - through a balance between helicity injection (or extraction) and resistive dissipation.

A computed field profile for a spherical FCS system is shown in Fig. 23 (Taylor and Turner, 1985). Analytic solutions for an idealisation in which the polar-caps are shrunk to polar points (though retaining finite flux through them) are shown in Fig. 24 (Turner, 1984). This illustrates some interesting changes which occur in the FCS configuration as the ratio

I_p/ψ_p , and hence μ , is increased. When I_p/ψ_p is much smaller than the lowest eigenvalue for the configuration ($\mu_s = 4.49/a$) , the externally linked flux (and current) forms a large part of the total flux (and current) in the system. As I_p/ψ_p approaches the eigenvalue μ_s the ratio of self-generated flux (and current) to the externally linked flux (and current) increases indefinitely and the externally linked flux is confined to a slim pencil along the axis of the plasma - which otherwise is identical to that in a simple Spheromak. As I_p/ψ_p increases beyond μ_s the configuration switches to one in which the externally linked flux passes around the <u>outside</u> of the Spheromak. [However, one would not expect this to be the lowest energy state when μ exceeds the lowest eigenvalue (see Section VII).].

The ratio of the self generated poloidal flux to the externally-linked flux defines a flux magnification ratio $M(\mu)$ which can be used to characterise FCS experiments in somewhat the same way that $F(\theta)$ (the toroidal field ratio) is used to characterise RFP experiments.

3. Experiments

Flux cored configurations have been produced in the PS-1 experiment (Bruhns et al., 1983) and in the CTX experiment (Jarboe, 1985; Jarboe et al., 1983). The latter experiment is particularly interesting as it has also demonstrated the sustainment of the Spheromak plasma by a voltage across the polar caps - though in a much distorted form. A schematic diagram of the configuration in the CTX sustained plasma is shown in Fig. 25. It can be seen that there is a core of flux (shown by hatched lines)

which passes from the inner electrode of the gun, along the axis of the Spheromak plasma and returns around it to the outer gun electrode. From the point of view of the plasma the gun-voltage therefore appears across the flux-core - though the "polar caps" are somewhat distant! The configuration shown has been sustained by the gun voltage for much longer than the normal resistive decay time of the magnetic fields.

Recognition that near relaxed state plasmas can be maintained in this way has opened up new possibilities and led to the investigation of configurations in which the source of helicity is still more distant from the plasma containment region (Jarboe, 1985). An example is shown in Fig. 26.

VII. STABILITY OF RELAXED STATES

It is clear that, because they are states of minimum energy, all relaxed states are stable against perturbations which leave helicity invariant. This includes all ideal magnetohydrodynamic perturbations.

The stability of the relaxed states was verified directly (Taylor, 1974b; see also Schmidt, 1966; Kruger, 1976a,b) by considering the second variation of magnetic energy, produced by a perturbation $\delta\underset{\sim}{A}$ about the equilibrium relaxed state,

$$\delta W_2 = \frac{1}{2}\int(\nabla \times \delta\underset{\sim}{A})^2 d\tau - \frac{\mu}{2}\int \delta\underset{\sim}{A}\cdot\nabla \times \delta\underset{\sim}{A}\, d\tau \quad . \tag{7.1}$$

If we use the normalisation

$$\frac{1}{2}\int(\nabla \times \delta\underset{\sim}{A})^2 d\tau = 1 \qquad (7.2)$$

and the boundary condition $\delta\underset{\sim}{A} = 0$, then the minimising perturbation satisfies

$$\nabla \times \nabla \times \delta\underset{\sim}{A} - \frac{\mu}{(1-g)} \nabla \times \delta\underset{\sim}{A} = 0 \quad . \qquad (7.3)$$

The corresponding perturbation in energy is

$$(\delta W_2)_{min} = \frac{g}{2}\int(\nabla \times \delta\underset{\sim}{A})^2 d\tau \qquad (7.4)$$

and is non-negative if $g \geq 0$. Comparing (7.3) with the eigenvalue equation (4.2) we see that $g \geq 0$ if $\mu \leq$ the lowest eigenvalue for the problem - as is the case for all minimum energy relaxed states.

Since this discussion does not require the fluid displacement $\underset{\sim}{\xi}$ to be finite it applies to resistive tearing modes as well as ideal modes (Taylor, 1976; Rosenbluth and Bussac, 1979). Consequently relaxed states are also stable to resistive tearing modes. This is illustrated by the result obtained (in Section III) for the large aspect ratio circular cross-section toroidal pinch. The point at which the lowest energy state ceases to be the axisymmetric configuration occurs at $\mu a = 3.11$. This is precisely the point at which the axisymmetric configuration becomes linearly unstable to a resistive tearing mode (Whiteman, 1962; Gibson and Whiteman, 1968).

[Ideal mhd instability does not arise until $\mu a = 3.18$ (Voslamber and Callebaut, 1962).]

As one would expect, therefore, the change from the symmetric relaxed state to the helical relaxed state corresponds to a bifurcation in which linear stability is transferred from one state to the other. However, it is important to realise that the theory of relaxed states goes beyond the linear theory. The helical deformation which occurs in the relaxed state is fully determined (by K/ψ^2) and in this respect the present theory provides a non-linear description of the resistive tearing mode (Martin and Taylor, 1974).

VIII. SUMMARY AND CONCLUSIONS

In this paper we have described the concept of plasma relaxation by reconnection of magnetic lines of force. This is brought about by plasma turbulence in the presence of small resistivity and leads to a unique lowest-energy relaxed state. We should emphasise that, because it is driven by turbulence, this relaxation occurs on a much shorter time scale than normal resistive diffusion. It is only on this shorter time scale that the magnetic helicity K is invariant. On the longer resistive time scale, energy and helicity will both decay unless deliberately sustained. Resistive decay usually causes the configuration to evolve away from the fully relaxed state and in that event periodic or continuous secondary relaxations occur to maintain the profile close to a relaxed configuration. Similar minor relaxations must occur when the discharge is sustained by helicity injection.

Another feature which should be emphasised is that relaxation is not a passive decay process. It involves the self generation of fields and currents by plasma turbulence, sometimes referred to as 'dynamo action'.

We have also described the calculation of the relaxed state in various systems. In all cases it satisfies Eq. (1.8), but the manner in which the appropriate solution is selected depends on the topology of the system and on the boundary conditions. Consequently there are several different types of relaxed state, each with its own distinct characteristics.

In parallel with the theoretical discussion we have reviewed some of the experimental evidence for relaxed states. Configurations close to those predicted are almost universally observed in Toroidal Pinches, in the Multipinch, in Spheromaks and in Flux Core Systems. [The well-known disruption in Tokamaks also appears to be an example of relaxation, in which the theory correctly predicts the negative voltage spike. However, apart from disruption, and sawtooth oscillation, relaxation does not play a dominant role in Tokamaks. This is presumably due to the strong toroidal magnetic field and the care taken to avoid mhd instability. This illustrates the point that some symmetry-breaking instability is necessary to initiate relaxation.]

The experiments provide quantitative verification of the distinct characteristics of the different types of relaxed state. These include such features as field reversal and current saturation in the Toroidal Pinch, and in a different form in the Multipinch, as well as flux annihilation and generation in the Spheromak and Flux Core Systems.

The remarkable success of the theory prompts investigation at a more detailed level. One question concerns the precise mechanism of relaxation and flux generation or dynamo action. This may be different in different circumstances - only the final state is unique. Theories of plasma turbulence are extensively discussed in the literature and in at least some cases lead to the relaxed state - but the subject is far from complete. The interested reader should see, for example, Moffatt (1978), Montgomery et al. (1978), Riyopoulos et al. (1982), Mattheus and Montgomery (1980), Ting et al. (1985), Frisch et al. (1975).

A related question is that of deviations from the fully relaxed profile. We have mentioned that in the RFP $\mu \equiv \underset{\sim}{j} \cdot \underset{\sim}{B}/B^2$ (which is uniform in a fully relaxed state) falls off in the vicinity of the wall. This is presumably due to the high plasma resistivity near the wall which the relaxation mechanism, or dynamo process, is unable fully to overcome. In investigating this, experiments of the Flux-Core type seem particularly relevant since one can control the relaxed state, change from one relaxed state to another by injecting helicity and, by having two pairs of electrodes instead of a single pair of polar caps, maintain a partially relaxed state.

ACKNOWLEDGMENT

I would like to thank my colleagues for many useful discussions on the topics in this paper. In particular, I am indebted to Torkil Jensen and M. S. Chu for valuable discussions on the general relaxed state, to R. La Haye for providing data on the Multipinch, to H. Yamada for data on the

S-1 Spheromak, and to H. Bodin and A. Newton for frequent guidance on toroidal pinch experiments. In addition D. Montgomery, L. Turner, T. Jarboe, A. Reiman, M. Bevir and C. Gimblett and others have provided helpful comment and criticism.

IX. APPENDIX

A. General theory of relaxed states

1. Toroidal Systems

The theory of relaxed states in a general toroidal system is similar to that for the large aspect ratio system described in Section III. The general theory has been discussed by Jensen and Chu (1984), whose description is followed in this section, but with some additional new features. A more mathematical view of some aspects of this problem can be found in Faber et al. (1982), (1985).

In a general toroidal system the relaxed state is found by minimising

$$W = \frac{1}{2} \int (\nabla \times \underset{\sim}{A})^2 d\tau \tag{9.1}$$

over all variations $\delta\underset{\sim}{A}$ of the vector potential which leave the helicity

$$K_0 = \int \underset{\sim}{A} \cdot \nabla \times \underset{\sim}{A} \, d\tau \tag{9.2}$$

invariant. Introducing a Lagrange multiplier this leads to

$$\delta I = \int \delta\underset{\sim}{A} \cdot [\nabla \times \nabla \times \underset{\sim}{A} - \mu \nabla \times \underset{\sim}{A}] + \oint \delta\underset{\sim}{A} \times (\nabla \times \underset{\sim}{A} - \frac{\mu \underset{\sim}{A}}{2}) \cdot dS \quad . \tag{9.3}$$

We assume that at the plasma-wall boundary the normal magnetic field

$(\underset{\sim}{n}\cdot\nabla \times \underset{\sim}{A})$ vanishes. This ensures that the helicity is gauge invariant (Section I C) and that δI is also gauge invariant (i.e. $\delta I \equiv 0$ if $\delta\underset{\sim}{A} = \nabla\phi$). If the wall is also perfectly conducting the condition $\underset{\sim}{E}_{\|}(\text{wall}) = 0$ implies that at the boundary $\delta\underset{\sim}{A}_{\|}$ is the gradient of a scalar. Writing $\delta\underset{\sim}{A} = \delta\underset{\sim}{A}^* + \nabla\phi$ where $\delta\underset{\sim}{A}^*_{\|}$ vanishes at the boundary, the minimisation (9.3) leads to the Euler equation:

$$\nabla \times \nabla \times \underset{\sim}{A} - \mu\nabla \times \underset{\sim}{A} = 0 \quad . \tag{9.4}$$

The specification of the relaxed state is completed by the boundary conditions $\underset{\sim}{n}\cdot\nabla \times \underset{\sim}{A} = 0$ and the given values of the loop integrals $\oint\underset{\sim}{A}\cdot d\underset{\sim}{\ell}$ and $\oint\underset{\sim}{A}\cdot d\underset{\sim}{s}$.

If we assume that the eigenfunction of the associated eigenvalue problem

$$\nabla \times \nabla \times \underset{\sim}{a}_i = \lambda_i \nabla \times \underset{\sim}{a}_i \quad , \tag{9.5}$$

with boundary condition $\underset{\sim}{a}_i = 0$, form a complete set then, following Jensen and Chu (1984), we may write

$$\underset{\sim}{A} = \underset{\sim}{A}_0 + \sum\alpha_i \underset{\sim}{a}_i \tag{9.6}$$

where $\underset{\sim}{A}_0$ represents a toroidal <u>vacuum</u> field satisfying the boundary conditions of the original problem. Note that an eigenfunction carries no toroidal flux and in an axisymmetric system the vacuum toroidal field will also be axisymmetric.

The eigenfunctions are orthogonal in the sense that

$$(\lambda_i - \lambda_j) \int \underset{\sim}{a}_i \cdot \nabla \times \underset{\sim}{a}_j = 0 \qquad (9.7)$$

but

$$\lambda_i \int \underset{\sim}{a}_i \cdot \nabla \times \underset{\sim}{a}_i = \int (\nabla \times \underset{\sim}{a}_i)^2 > 0 \qquad (9.8)$$

so that the appropriate normalisation is

$$\int \underset{\sim}{a}_i \cdot \nabla \times \underset{\sim}{a}_j = \int \underset{\sim}{a}_j \cdot \nabla \times \underset{\sim}{a}_i = \frac{\lambda_i}{|\lambda_i|} \delta_{ij} \quad . \qquad (9.9)$$

Then, so long as μ is not equal to an eigenvalue, the coefficients α_i are given by

$$\alpha_i = \frac{\mu}{(\lambda_i - \mu)} \frac{|\lambda_i|}{\lambda_i} I_i \qquad (9.10)$$

where

$$I_i = \int \underset{\sim}{a}_i \cdot \nabla \times \underset{\sim}{A}_0 \qquad (9.11)$$

and the important invariant quantity K/ϕ^2 can be expressed as

$$\frac{K}{\phi^2} = \frac{1}{\phi^2} \int \underset{\sim}{A}_0 \cdot \nabla \times \underset{\sim}{A}_0 + \sum_i \frac{\lambda_i}{|\lambda_i|} \frac{I^2}{\phi^2} \left\{ \frac{\lambda_i^2}{(\lambda_i - \mu)^2} - 1 \right\} \quad . \qquad (9.12)$$

This expression depends only on the shape of the toroidal container. It constitutes a relation between K/ψ^2 and the parameter μ. Note that K/ψ^2 diverges when $\mu \to \lambda_i$ unless $I_i = 0$.

At this point, we depart from Jensen and Chu to recognise that many eigenfunctions may not appear in the expansion (9.6). For example, in an axisymmetric system all non-axisymmetric eigenfunctions ($\sim \exp in\phi$ with $n \neq 0$) are absent since for them $I_i \equiv 0$. Similarly in the Multipinch, I_i also vanishes even for axisymmetric eigenfunctions when these are anti-symmetric about the mid plane of the cross-section. The eigenfunctions for which $I_i \equiv 0$ will be termed decoupled.

With this in mind, we see that in axisymmetric systems the solution

$$\underset{\sim}{A} = \underset{\sim}{A}_0 + \sum_i{}' \frac{\mu}{(\lambda_i - \mu)} \frac{\lambda_i}{|\lambda_i|} I_i \underset{\sim}{a}_i \qquad (9.13)$$

(where $\sum'$ denotes a sum over coupled eigenfunctions only) represents a solution analogous to the $m = 0$, $k = 0$, type I, solution in the circular cross-section torus. For this solution μ is determined, through Eq. (9.12), by the value of K/ψ^2; such a solution can always be found for some value of μ in the range $\lambda_1^- < \mu < \lambda_1^+$, where λ_1^- is the largest negative eigenvalue and λ_1^+ is the smallest positive eigenvalue. For a system which has mirror symmetry about any plane the eigenvalues occur in pairs, $\pm \lambda_i$; consequently it is often sufficient to discuss only positive eigenvalues.

When μ is equal to one of the decoupled eigenvalues λ_j, an arbitrary multiple of the corresponding decoupled eigenfunction can be added to (9.13) and it will remain a solution of Eq. (9.4) satisfying the boundary conditions. Thus another solution is given by

$$\underset{\sim}{A} = \underset{\sim}{A}_0 + \sum_{i\neq j}{}' \frac{\lambda_i \lambda_j}{|\lambda_i| (\lambda_i - \lambda_j)} I_i \underset{\sim}{a}_i + \beta \underset{\sim}{a}_j \qquad (9.14)$$

where the sum is again over coupled eigenfunctions only. This solution is valid only for $\mu = \lambda_j$ and K/ψ^2, now given by

$$\frac{K}{\psi^2} = \frac{1}{\psi^2} \int (\underset{\sim}{A}_0 \cdot \nabla \times \underset{\sim}{A}_0) d\tau + \sum_{i\neq j} \frac{\lambda_i}{|\lambda_i|} \frac{I_i^2}{\psi^2} \frac{(2\lambda_i - \lambda_j)}{(\lambda_i - \lambda_j)^2} + \frac{\beta^2}{\psi^2} \frac{\lambda_j}{|\lambda_j|} , \qquad (9.15)$$

determines the coefficient β. These solutions are analogous to the type II, mixed, solutions of the circular plasma.

Noting that the lowest energy solution is that with the smallest $|\mu|$ (see below), we can now summarise the general relaxed states of axisymmetric systems as follows. (For simplicity we consider that μ, and K are positive and the expression 'lowest eigenfunction' means that with the smallest positive eigenvalue.)

If the lowest eigenfunction is decoupled then there are two candidates for the lowest energy relaxed state. The first exists for a continuous range of μ, from zero to the lowest eigenvalue λ_0. It is the appropriate solution when K/ψ^2 is small and μ is then determined by, and increases with, K/ψ^2. The second candidate is a superposition

of the first solution and the lowest eigenfunction. It exists only for $\mu = \lambda_0$ and is the appropriate solution when K/ψ^2 is such that μ would exceed λ_0 in the first solution. In this event μ remains at λ_0 and is no longer determined by K/ψ^2 ; instead K/ψ^2 determines the amplitude of the eigenfunction component. In this solution the current, at fixed toroidal flux, saturates with increasing Volt-seconds.

As we have noted, in axisymmetric systems the lowest eigenfunction is usually decoupled and the above description applies. If the lowest eigenfunction is <u>not</u> decoupled then only the first solution exists and μ is <u>always</u> determined by K/ψ^2. However, as the lowest eigenvalue is approached $K/\psi^2 \to \infty$, so that even in this situation μ can never exceed the lowest eigenvalue (Jensen and Chu, 1984). In this regard, therefore, there is little distinction between the behaviour of systems whose lowest eigenfunction is decoupled and those in which it is coupled - especially if the coupling is weak.

2. Spherical systems (e.g. Spheromak)

For a general (topologically) spherical system whose boundary is a flux surface, the relaxed state is again given by Eq. (9.4). However, a spherical system is singly connected and all loop integrals $\oint \underset{\sim}{A} \cdot d\underset{\sim}{s}$ are zero. Apart from a gauge transformation this is equivalent to $\underset{\sim}{A} = 0$ on the boundary so that the <u>only</u> relaxed states in spherical systems are the eigenfunctions. The lowest energy relaxed state is just the lowest eigenfunction. Consequently, as noted in section VI, μ and the field

profiles are determined by the shape of the container alone. The invariant K determines only the magnitude of the field and there is no invariant toroidal flux.

B. Lowest energy vs. μ

In determining the lowest energy relaxed state, there is a useful relation between the difference in energy of two states of given helicity and the difference in μ for the two states (Taylor, 1975; Martin and Taylor, 1974; Faber et al., 1982; Reimann, 1980, 1981).

Suppose we have two solutions $\underset{\sim}{A}_1$ and $\underset{\sim}{A}_2$ (corresponding to μ_1 and μ_2) of Eq. (9.4) which have the same helicity K and satisfy the same boundary conditions. Then apart from a gauge transformation $\underset{\sim}{A}_1 = \underset{\sim}{A}_2$ on the boundary and consequently one can verify the following identities:

$$\int[\nabla \times (\underset{\sim}{A}_2 - \underset{\sim}{A}_1)]^2 = (\mu_2 + \mu_1) \int(\underset{\sim}{A}_2 - \underset{\sim}{A}_1)\cdot\nabla \times \underset{\sim}{A}_2 \qquad (9.16)$$

$$\int(\nabla \times \underset{\sim}{A}_2)^2 - \int(\nabla \times \underset{\sim}{A}_1)^2 = (\mu_2 - \mu_1) \int(\underset{\sim}{A}_2 - \underset{\sim}{A}_1)\cdot\nabla \times \underset{\sim}{A}_2 \ . \qquad (9.17)$$

Consequently, if W_1 and W_2 denote the energy of the two solutions,

$$W_2 - W_1 = \frac{(\mu_2 - \mu_1)}{(\mu_2 + \mu_1)} \int \frac{(B_2 - B_1)^2}{2} \ , \qquad (9.18)$$

or

$$W_2 - W_1 = \frac{(\mu_2^2 - \mu_1^2)}{(\mu_2 + \mu_1)} \int \frac{(B_2 - B_1)^2}{2} \quad . \tag{9.19}$$

Consequently, if there are two possible relaxed states [i.e. two solutions of Eq. (9.4) with correct helicity] then the lower energy one is that with the smaller $|\mu|$.

REFERENCES

Antoni, V., S. Martini, S. Ortolani, and R. Paccagnella, 1983, in Proc. Workshop on Mirror Based and Field Reversed Magnetic Fusion, Varenna, pp. 107-133.

Berger, M. A., and G. B. Field, 1984, J. Fluid Mech. 147, 133.

Bevir, M., and J. Gray, 1980, in Proc. Reverse Field Pinch Theory Workshop, edited by H. R. Lewis and R. A. Gerwin (Los Alamos National Laboratory), Vol III, paper A-3.

Bhattacharjee, A., R. L. Dewar, and D. Monticello, 1980, Phys. Rev. Lett. 45, 347.

Bhattacharjee, A., and R. L. Dewar, 1982, Phys. Fluids 25, 887.

Bodin, H. A. B., and A. A. Newton, 1980, Nucl. Fusion 20, 1255.

Bodin, H. A. B., 1984, Proc. ICPP Invited Papers, Lausanne, Vol. I, p. 417.

Bondeson, A., G. Marklin, Z. G. An, H. H. Chen, Y. C. Lee, and C. S. Liu, 1981, Phys. Fluids 24, 1682.

Bruhns, H., C. Chin-Fatt, Y. P. Chong, A. W. DeSilva, G. C. Goldenbaum, H. R. Griem, G. W. Hart, R. A. Hess, J. H. Irby, and R. S. Shaw, 1983, Phys. Fluids 26, 1616.

Bruhns, H., G. Raupp, K. Sobel, J. Steiger, and A. Weichelt, 1984, Proc. Symposium on Compact Toroid Research, Princeton, pp. 25-28.

Butt E. P., C. W. Gowers, A. Mohri, A. A. Newton, D. C. Robinson, A. J. L. Verhage, M. R. C. Watts, Li Yin-An, and H. A. B. Bodin, 1975, Proc. 7th Europ. Conf. on Cont. Fusion & Plasma Phys., Lausanne, Vol. I, p. 39.

Chandrasekhar, S., and P. C. Kendall, 1957, Astrophys. J. 126, 457.

DiMarco, J. N., 1983, Proc. Course on Mirror Based & Field Reversed Magnetic Fusion, Varenna, Vol. II, p. 681.

Edenstrasse, J. W., and W. Schuurman, 1983, Phys. Fluids 26, 500.

Faber, V., A. B. White, and G. M. Wing, 1982, J. Math. Phys. 23, 1524.

Faber, V., A. B. White, and G. M. Wing, 1985, Plasma Phys. & Cont. Fusion 27, 509.

Finn, J. M., W. M. Mannheimer, and E. Ott, 1981, Phys. Fluids 24, 1336.

Frisch, U., A. Pouquet, J. Léorat, and A. Mazure, 1975, J. Fluid Mech. 68, 769.

Furth, H., J. Killeen, and M. N. Rosenbluth, 1963, Phys. Fluids 6, 459.

Furth, H. P., 1981, J. Vac. Sci. Technol. 18, 1073.

Furth, H., 1985, Phys. Fluids 28, 1595.

Gibson, R. D., and K. Whiteman, 1968, Plasma Phys. 10, 1101.

Goldenbaum, G. C., J. H. Irby, Y. P. Chong, and G. W. Hart, 1980, Phys. Rev. Lett. 44, 393.

Goldenbaum, G. C., 1982, Physica Scripta T2/2, 359.

Hameiri, E., and J. H. Hammer, 1982, Phys. Fluids 25, 1855.

Hart, G. W., A. Janos, D. D. Meyerhofer, and M. Yamada, 1985, Princeton Laboratory Report PPPL 2257. Submitted to Phys. Fluids.

Hasegawa, A., 1985, Advances in Physics 34, 1.

Heyvaerts, J., and E. R. Priest, 1984, Astron. Astrophys. 137, 63.

Janos, A., G. W. Hart, and M. Yamada, 1985, Princeton Laboratory Report PPPL 2231. Submitted to Phys. Rev. Lett.

Jarboe, T. R., I. Henins, H. W. Hoida, R. K. Linford, J. Marshall, D. A. Platts, and A. R. Sherwood, 1980, Phys. Rev. Lett. 45, 1264.

Jarboe, T. R., I. Henins, A. R. Sherwood, Cris W. Barnes, and H. W. Hoida, 1983, Phys. Rev. Lett. 51, 39.

Jarboe, T. R., Cris W. Barnes, I. Henins, H. W. Hoida, S. O. Knox, R. K. Linford, and A. R. Sherwood, 1984, Phys. Fluids 27, 13.

Jarboe, T. R., 1985, Comments on Plasma Phys. 9, 161.

Jensen, T., and M. S. Chu, 1981, J. Plasma Phys. 25, 459.

Jensen, T., and M. S. Chu, 1983, in Proc. 5th Symposium on Phys. and Tech. of Compact Toroids, edited by A. L. Hoffman and R. D. Milroy, pp. 174-177.

Jensen, T., and M. S. Chu, 1984, Phys. Fluids 27, 2881.

Katsurai et al., 1984, Spheromak Researches in the University of Tokyo, Proc. 6th US-Japan CT Symposium, Hiroshima.

Kawai, K., and Pietrzyk, A. A., 1981, Bull. Am. Phys. Soc. 26, 905.

Kondoh, Y., 1981, Nucl. Fusion 21, 1607.

Konigl, A., and A. R. Choudhuri, 1985, Astrophys. J., 289, 173.

Krüger, J., 1976a, J. Plasma Phys. 15, 15.

Kruger, J., 1976b, J. Plasma Phys. 15, 31.

Kruskal, M. D., and R. M. Kulsrud, 1958, Phys. Fluids 1, 265.

La Haye, R. J., P. S. C. Lee, R. W. Moore, and T. Ohkawa, 1984, Bull. Am. Phys. Soc. 29, 1331.

La Haye, R. J., T. H. Jensen, P. S. C. Lee, R. W. Moore, and T. Ohkawa, 1985, GA Technologies Report GA-A17956. Submitted to Phys. Fluids.

Mannheimer, W., 1981, Phys. Fluids 24, 986.

Martin, T. J., and J. B. Taylor, 1974, unpublished Culham Laboratory Report.

Mattheus, W. H., and D. C. Montgomery, 1980, in Proc. Reverse Field Pinch Theory Workshop, edited by H. R. Lewis and R. A. Gerwin (Los Alamos National Laboratory).

Moffatt, H. K., 1978, Magnetic Field Generation in Electrically Conducting Fluids (Cambridge Univ. Press, New York).

Montgomery, D., L. Turner, and G. Vahala, 1978, Phys. Fluids, 21, 757.

Nagata, M., Y. Honda, K. Ikegami, M. Nishikawa, A. Ozaki, N. Satomi, T. Uyama, and K. Watanabe, 1984, in Plasma Phys. & Cont. Nucl. Fusion Research, Proc. 10th IAEA Conference, London, Vol. II, p. 655.

Newton, A. A., 1985, private communication.

Nogi, Y., H. Ogura, Y. Osanai, K. Saito, S. Shiina, H. Yoshimura, 1980, J. Phys. Soc. Japan 49, 710.

Ohkawa T., M. Chu, C. Chu, and M. Schaffer, 1980, Nucl. Fusion 20, 1464.

Ortolani, S., and G. Rostagni, 1983, Nuc. Instrum. & Methods, 207, 35.

Ortolani, S., 1984, in Twenty Years of Plasma Physics, Proc. ICTP Trieste Meeting, edited by B. McNamara, p. 75.

Parker, E. N., 1957, J. Geophys. Res. 62, 509.

Petschek, H. E., 1965, AAS-NASA Symposium on Physics of Solar Flairs, NASA publication Sp50.

Reiman, A., 1980, Phys. Fluids 23, 230.

Reiman, A., 1981, Phys. Fluids 24, 956.

Riyopoulos, S., A. Bondeson, and D. Montgomery, 1982, Phys. Fluids 25, 107.

Rosenbluth, M. N., and M. N. Bussac, 1979, Nucl. Fusion 19, 489.

Rusbridge, M. G., 1977, Plasma Phys. 19, 499.

Rusbridge, M. G., 1982, Nucl. Fusion 22, 1291.

Schmidt, G., 1966, Physics of High Temperature Plasmas, (Academic Press).

Sweet, P. A., 1958, Electromagnetic Phenomena in Cosmical Physics (Cambridge Univ. Press, New York).

Tamano, T., T. Carlstrom, C. Chu, R. Goforth, G. Jackson, R. La Haye, T. Ohkawa, M. Schaffer, and P. Taylor, 1983, in Proc. Course on Mirror Based and Field Reversed Magnetic Fusion, Varenna, Vol. II, p. 653.

Tamaru, T., K. Sugisaki, K. Hayase, T. Shimada, Y. Hirano, Y. Maejima, K. Ogawa, K. Hirano, S. Kitagawa, K. Sato, M. Wakatani, S. Yamada, H. Arimoto, Y. Kita, S. Yamaguchi, A. Nagata, S. Ido, and I. Kawakami, 1978, Plasma Phys. & Contr. Nuclear Fusion Research, Proc. 7th IAEA Conference, Innsbruck, Vol. II, pp. 55-68.

Taylor, J. B., 1974a, Phys. Rev. Lett. 33, 1139.

Taylor, J. B., 1974b, unpublished.

Taylor, J. B., 1975, in Plasma Phys. & Cont. Nucl. Fusion Research, Proc. 5th IAEA Conference, Tokyo, Vol. I, p. 161.

Taylor, J. B., 1976, in Pulsed High Beta Plasmas, edited by D. E. Evans (Pergamon Press, Oxford and New York) p. 59.

Taylor, J. B., 1980, in Proc. Reverse Field Pinch Theory Workshop, edited by H. R. Lewis and R. A. Gerwin (Los Alamos National Laboratory), Vol. V.

Taylor, J. B., and M. F. Turner, 1985, unpublished.

Ting, A. C., W. H. Matthews, and D. Montgomery, 1985. Submitted to Phys. Fluids.

Toyama, H., N. Asakura, K. Hattori, N. Inoue, S. Ishida, S. Matsuzuka, K. Miyamoto, J. Morikawa, Y. Nagayama, H. Nihei, S. Shinohara, Y. Ueda, K. Yamagishi, and Z. Yoshida, 1985, Proc. 12th European Conf. on Cont. Fusion & Plasma Phys., Budapest, Vol. I, p. 602.

Turner, L., and J. P. Christiansen, 1981, Phys. Fluids 24, 893.

Turner, L., 1984, Phys. Fluids 27, 1677.

Turner, W. C., E. H. A. Granneman, C. W. Hartman, D. S. Prono, J. Taska, and A. C. Smith, Jr., 1981, J. Appl. Phys. 52, 175.

Turner, W. C., G. C. Goldenbaum, E. H. A. Granneman, J. H. Hammer, C. W. Hartman, D. S. Prono, and J. Taska, 1983, Phys. Fluids 26, 1965.

Vasyliunas, V. M., 1975, Res. Geophys. and Space Phys. 13, 303.

Verhage, A. J. L., A. S. Furzer, and D. C. Robinson, 1978, Nucl. Fusion 18, 457.

Voslamber, D., and D. K. Callebaut, 1962, Phys. Rev. 128, 2016.

Watt, R. G., and R. A. Nebel, 1983, Phys. Fluids 26, 1168.

Watt, R. G., J. A. Phillips, and A. A. Newton, 1985, to be published.

Wells, D. R., and J. Norwood, 1969, J. Plasma Phys. 3, 21.

White, R. B., 1983, Handbook of Plasma Physics (North Holland, Amsterdam).

Whiteman, K., 1962, Plasma Phys. 7, 293.

Woltjer, L., 1958, Proc. Nat. Acad. Sci. 44, 489.

Yamada, M., H. P. Furth, W. Hsu, A. Janos, S. Jardin, M. Okabayashi, J. Sinnis, T. H. Stix, and K. Yamazaki, 1981, Phys. Rev. Lett. 46, 188.

Yamada, M., R. Ellis Jr., H. P. Furth, G. Hart, A. Janos, S. Jardin, F. Levinton, D. Meyerhofer, M. Mimura, C. H. Nam, S. Paul, A. Sperduti, S. Von Goeler, F. Wysocki, and P. Young, 1984, in Plasma Phys. & Cont. Nucl. Fusion Research, Proc. 10th IAEA Conference, London.

TABLE I. Toroidal pinch experiments.

Representative parameters[a].

	ZETA	ALPHA	ETA-BETA	TPE-IR(M)	ZT-40(M)	OHTE	HBTX-1A	REP
R[m]	1.50	1.60	0.65	0.5	1.14	1.24	0.8	0
a[m]	0.50	0.50	0.125	0.09	0.20	0.19	0.26	0
I[kA]	350	-	180	130	190	230	200	2
$I_{(max)}$	900	300	280	-	440	500	500	2
T_e[eV]	200	-	40	300	150	75	50	
$n[10^{20}m^{-3}]$	-	-	2	0.3	0.25	0.4	0.2	0

[a] Based on table prepared by Ortolani and Rostagni (1983) with additional data fro
Bodin and Newton (1980), Watt et al. (1985), and Toyama et al. (1985).

TABLE II. Spheromak experiments. Representative parameters.

	PS-1[a]	CTX[b]	S-1[c]	BETA II[d]	CTCC-1[e]	HSE[f]	CθP[g]	TODAI[h]
Flux container (cm)	6×14	30×40	30×55	40×40	20×25	6×9	4×8	10×15
I_{max}(kA)	130	500	300	330	100	240	20	80
T_e(eV)	-	150	110	10	40	10	10	-

[a] Goldenbaum et al. (1980).

[b] Jarboe et al. (1980); Jarboe et al. (1984).

[c] Yamada et al. (1981); Yamada et al. (1984).

[d] Turner et al. (1983).

[e] Nagata et al. (1984).

[f] Bruhns et al. (1984).

[g] Kawai and Pietrzyk (1981).

[h] Katsurai et al. (1984).

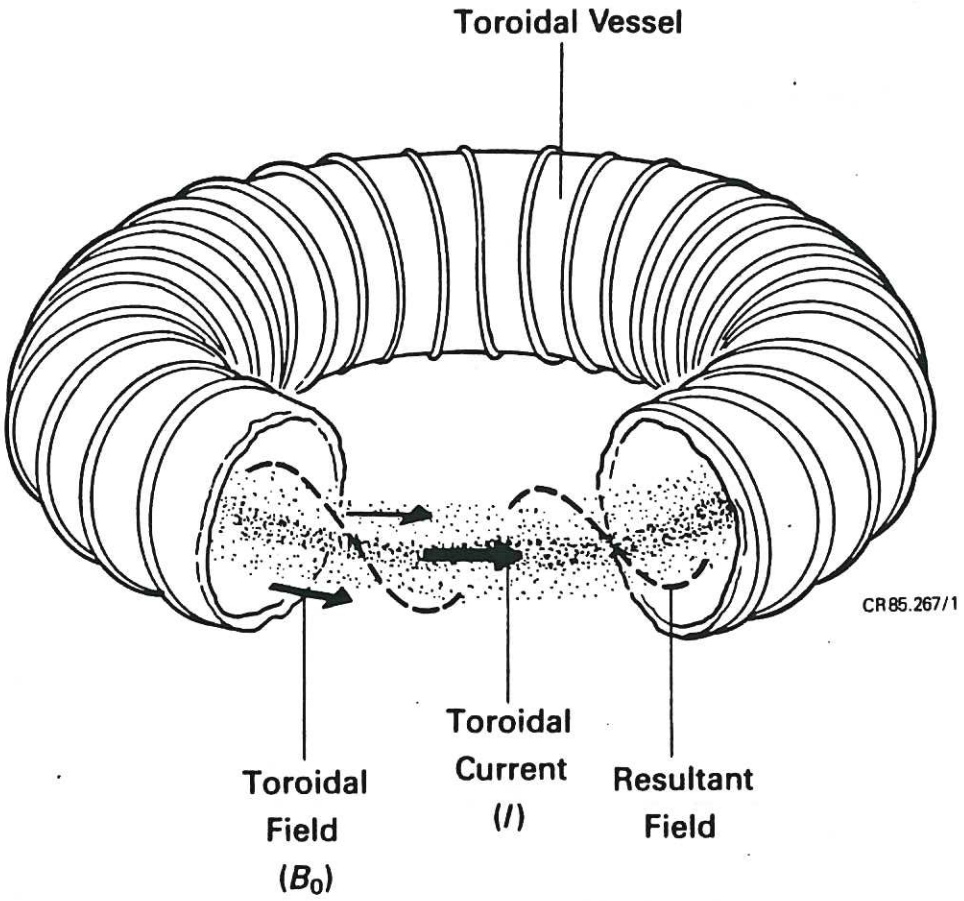

FIG. 1. The toroidal pinch.

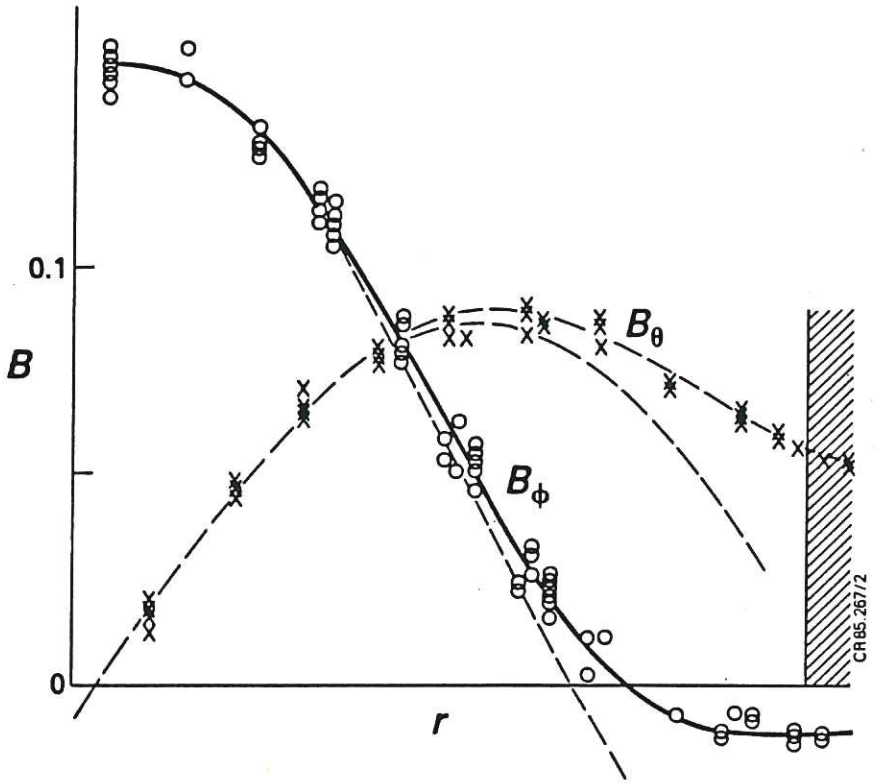

FIG. 2. Experimental and theoretical magnetic field profiles.

HBTX1A.
(From Bodin, 1984.)

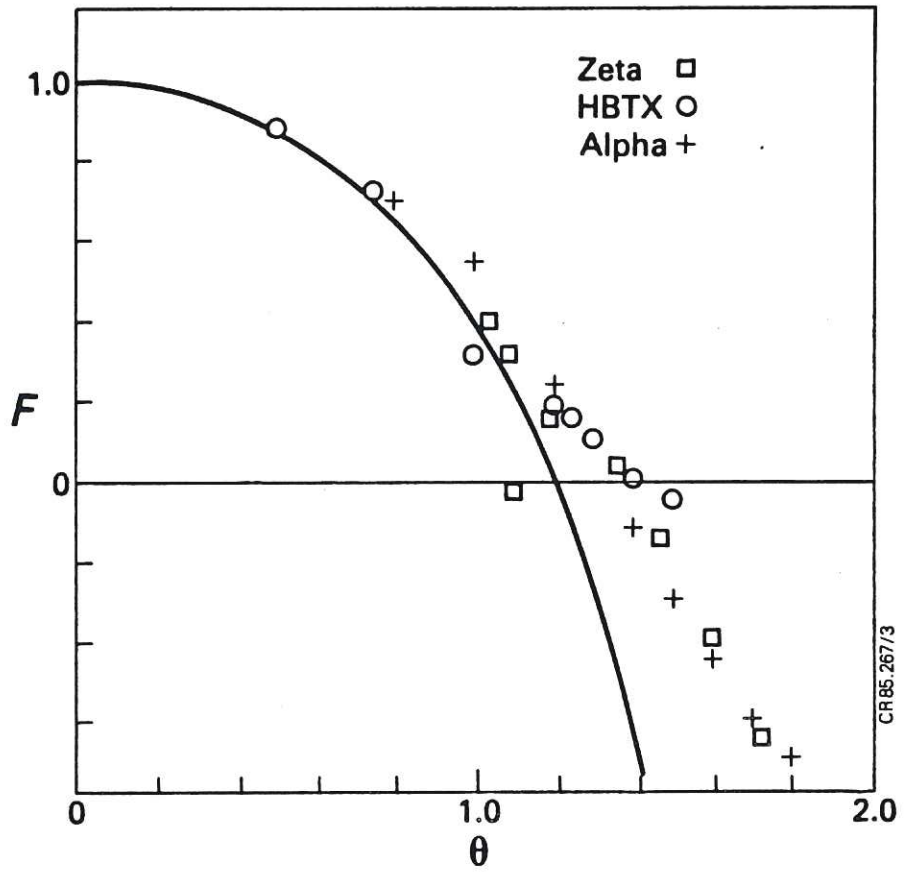

FIG. 3. F-θ diagram. Data from HBTX1, ALPHA, and ZETA and theoretical curve.

(From Bodin and Newton, 1980.)

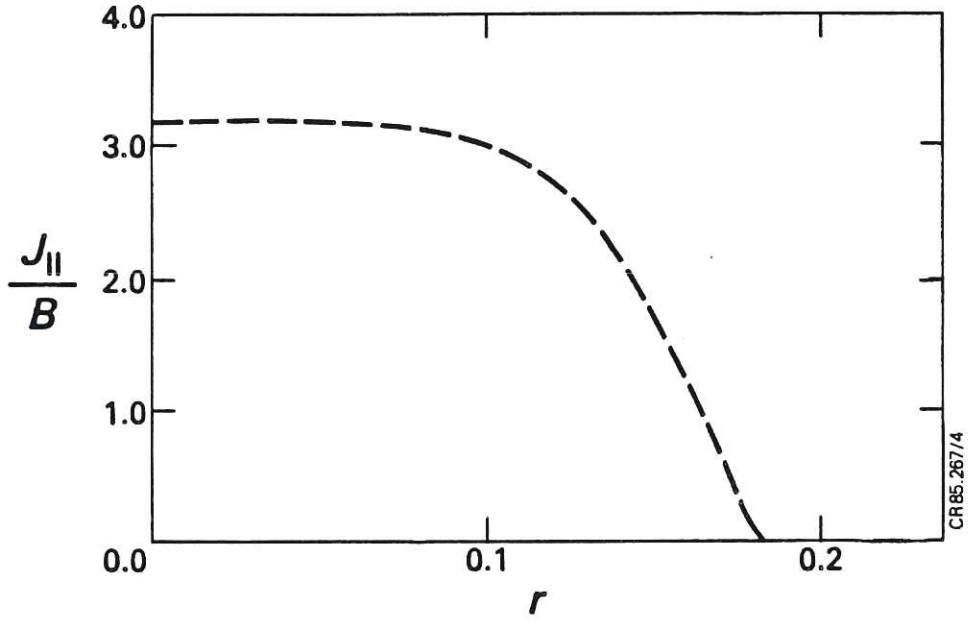

FIG. 4. Measured profile of μ(r). OHTE.

(From Tamano et al., 1983.)

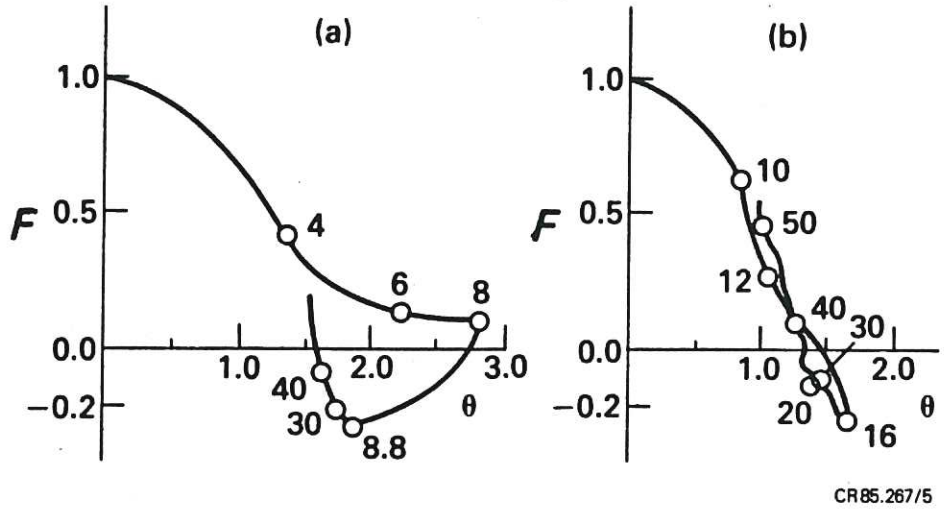

FIG. 5. Time dependent F-θ curve for HBTX1. Times in μsec.

(a) Fast mode.

(b) Slow mode.

(From Bodin and Newton, 1980.)

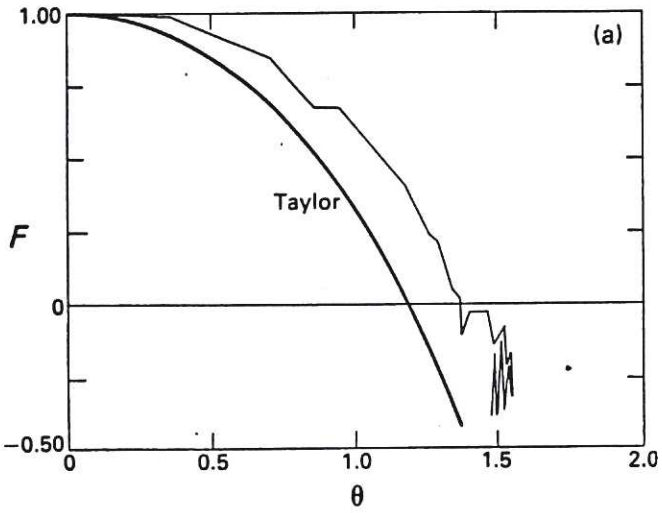

FIG. 6(a) Time dependent F-θ curve. ZT-40 experiment. (From DiMarco, 1983).

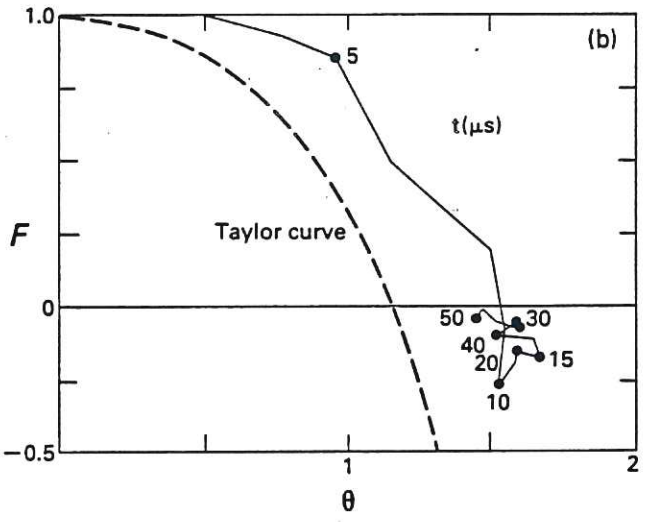

FIG. 6(b) Time dependent F-θ curve. TPRE experiment. (From Tamura et al., 1978).

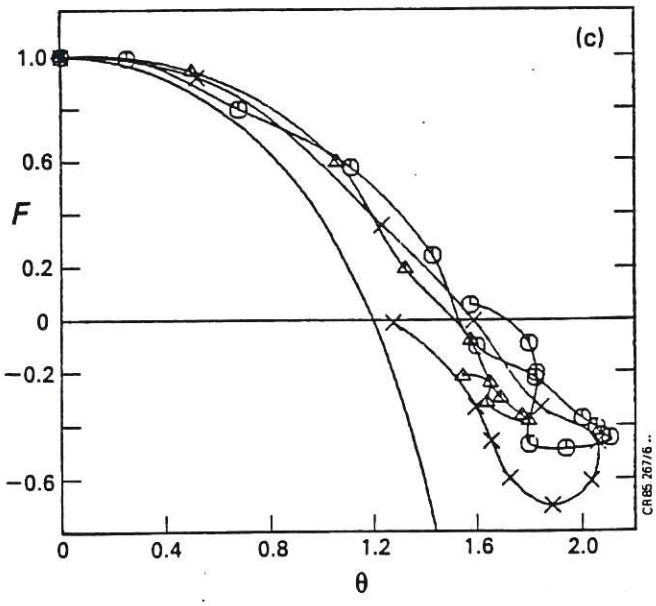

FIG. 6(c) Time dependent F-θ curve. REPUTE experiment. (From Toyama et al., 1985).

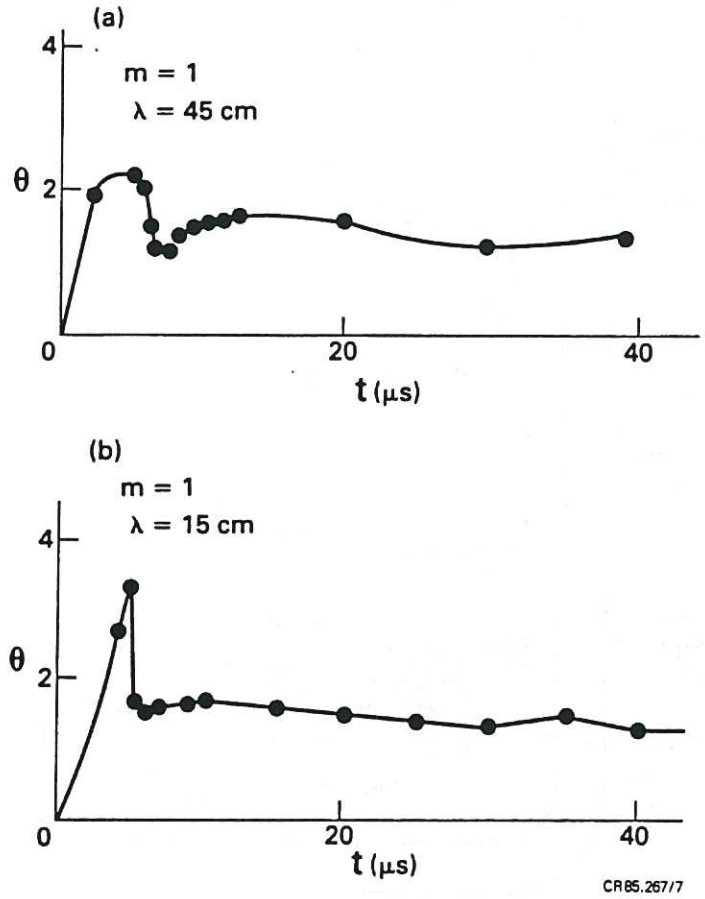

FIG. 7. Limitation of θ. HBTX1.

(From Bodin and Newton, 1980.)

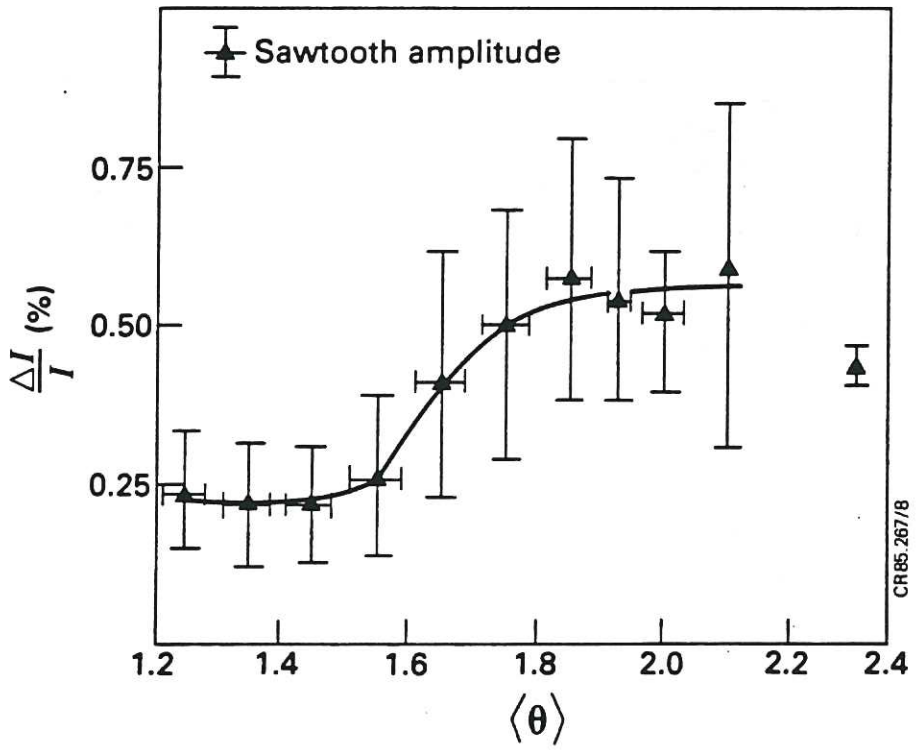

FIG. 8. Fluctuation level vs. θ. ZT-40.

(From Watt and Nebel, 1983.)

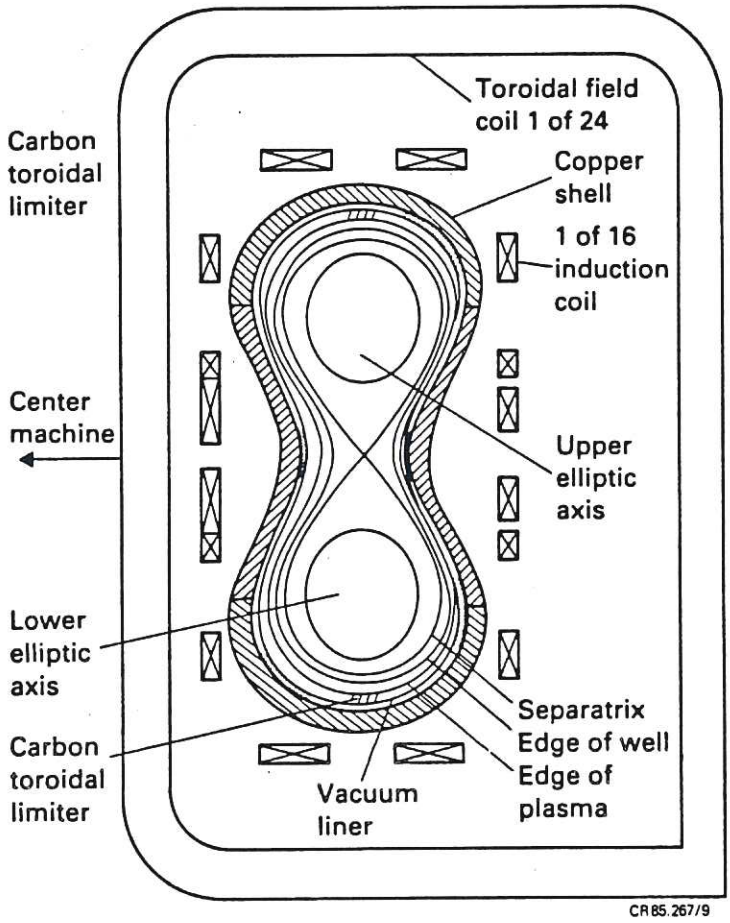

FIG. 9. Multipinch experiment.

(From La Haye et al., 1985.)

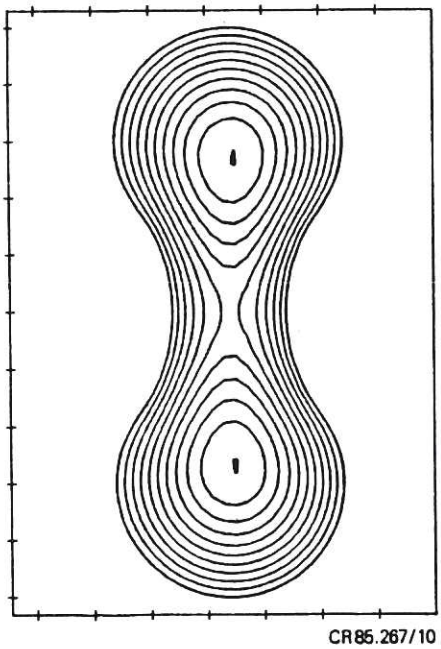

FIG. 10. Relaxed profile in Multipinch. $\mu a = 1.5$.

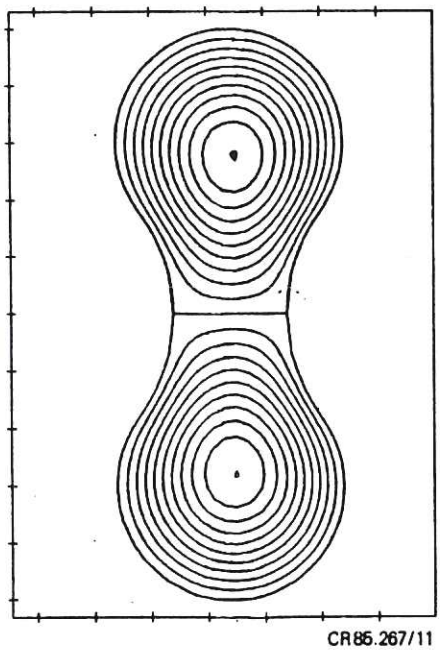

FIG. 11. Eigenfunction for Multipinch. $\mu a = 2.21$.

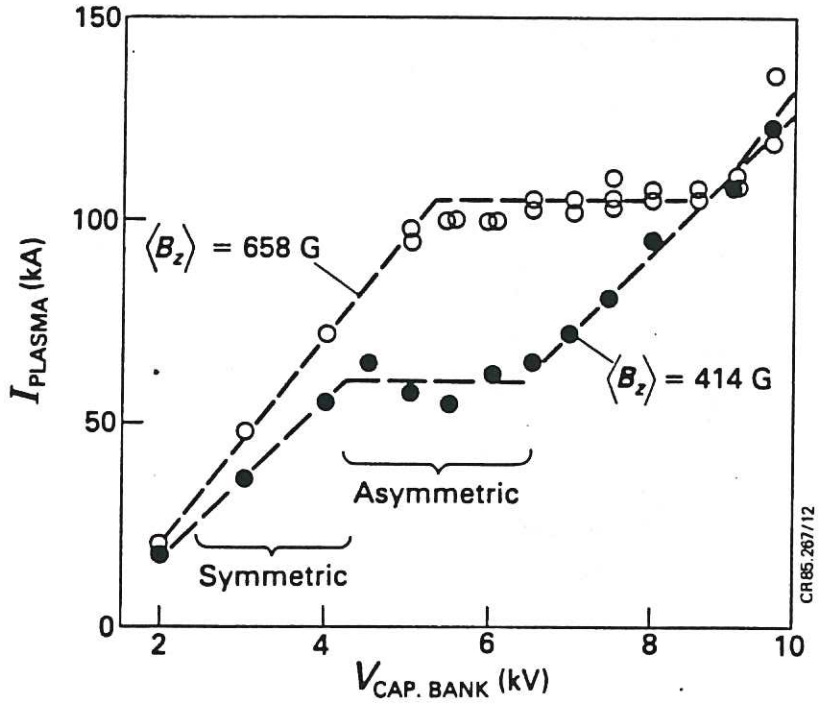

FIG. 12. Plasma current vs. driving voltage in Multipinch.

(From La Haye et al., 1985.)

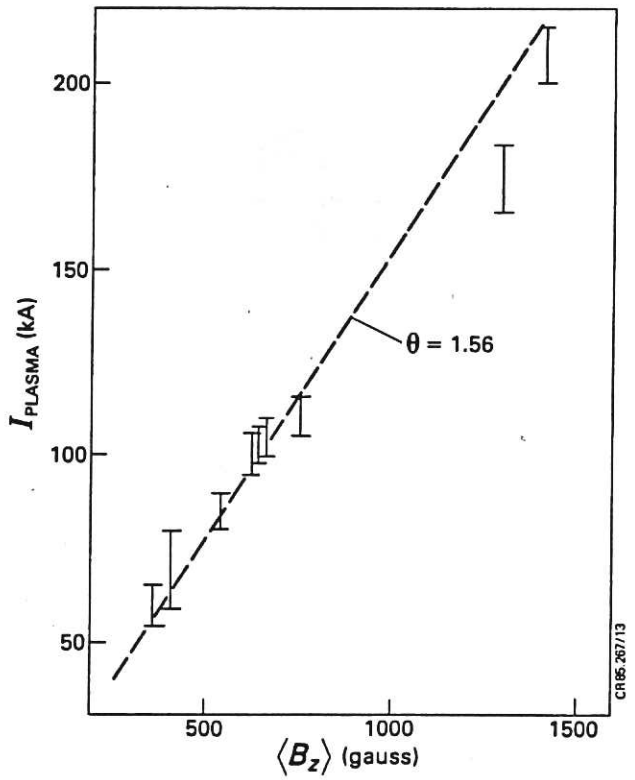

FIG. 13. Variation of I_{sat} with toroidal flux in Multipinch.

(N.B. θ = 1.56 corresponds to μa = 2.42 in this configuration.)

(From La Haye et al., 1985.)

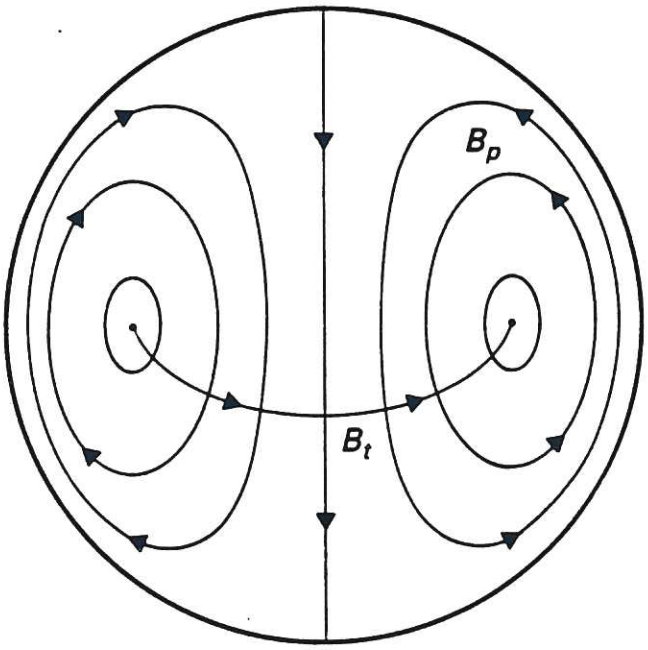

CR85.267/14

FIG. 14. Spheromak configuration. Schematic.

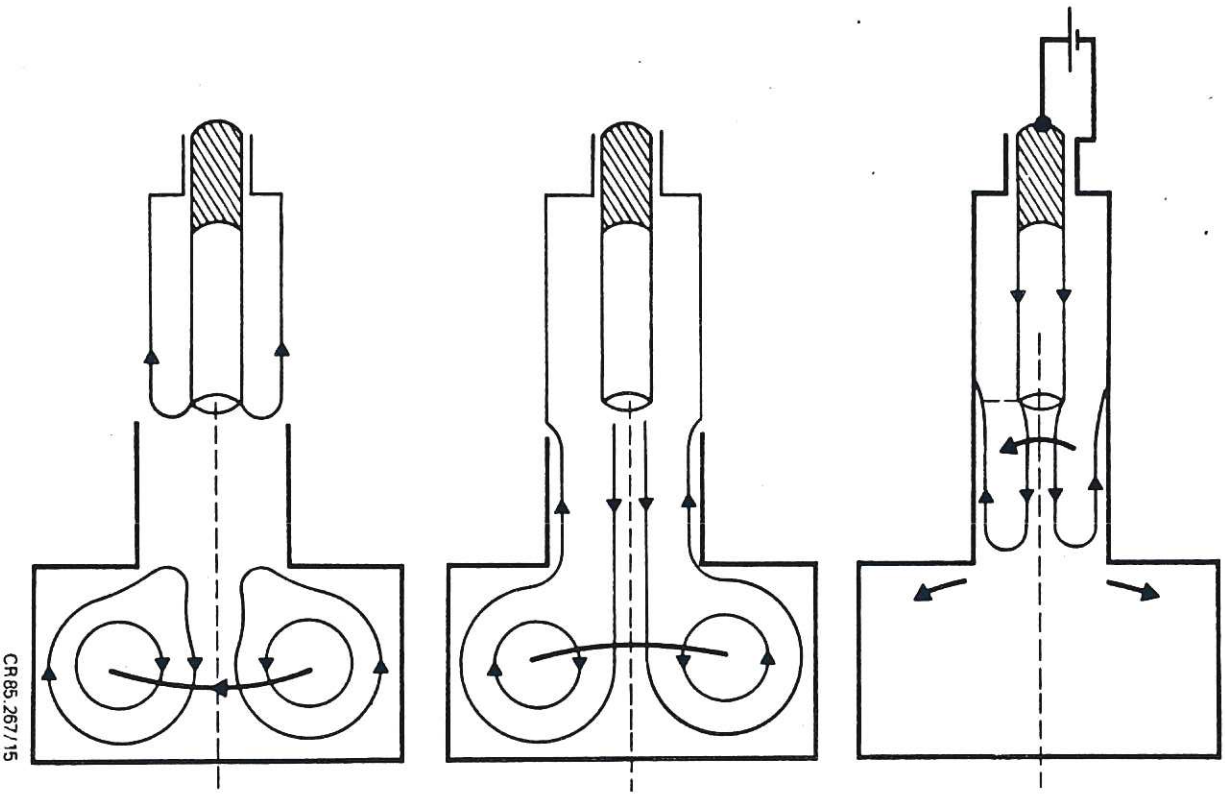

CR85.267/15

FIG. 15. Spheromak formation by plasma gun.

(From Turner et al., 1983.)

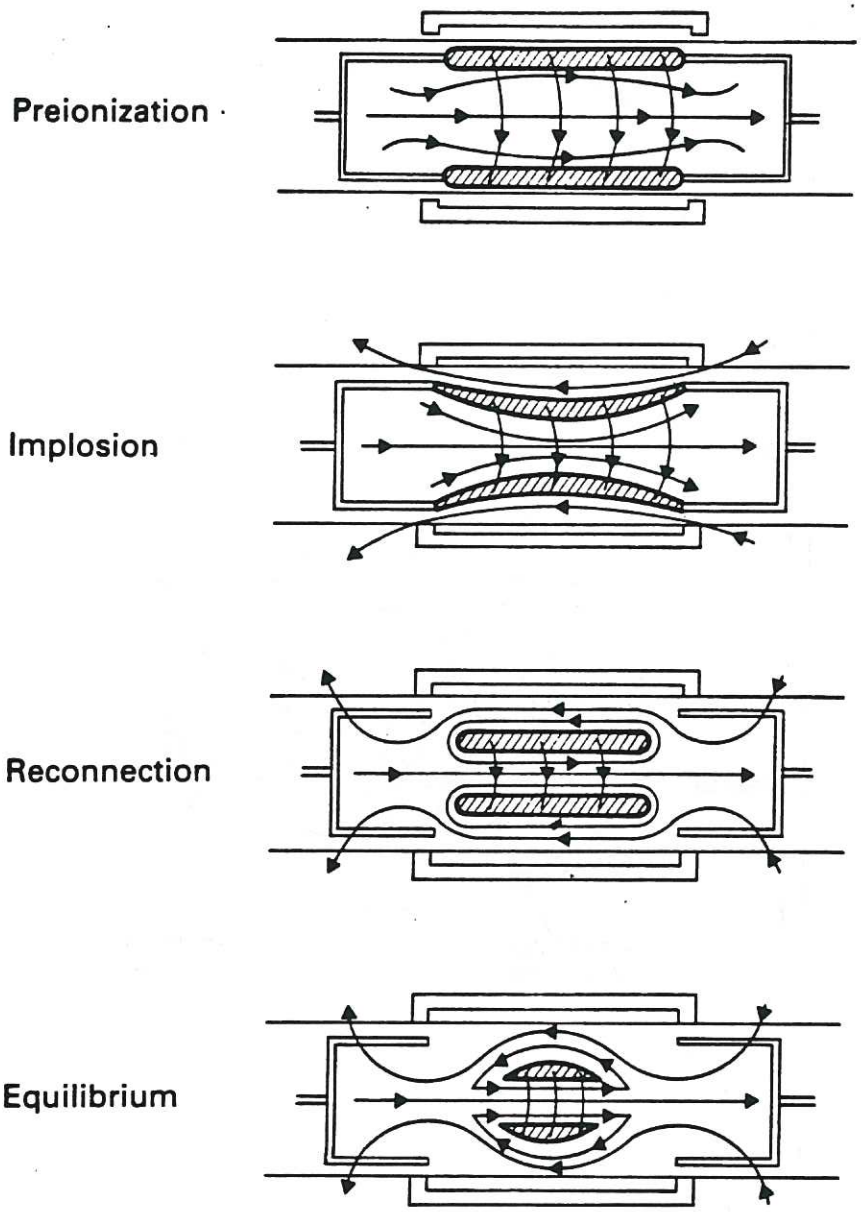

FIG. 16. Spheromak formation by combined θ-z discharge.

(From Goldenbaum et al., 1980.)

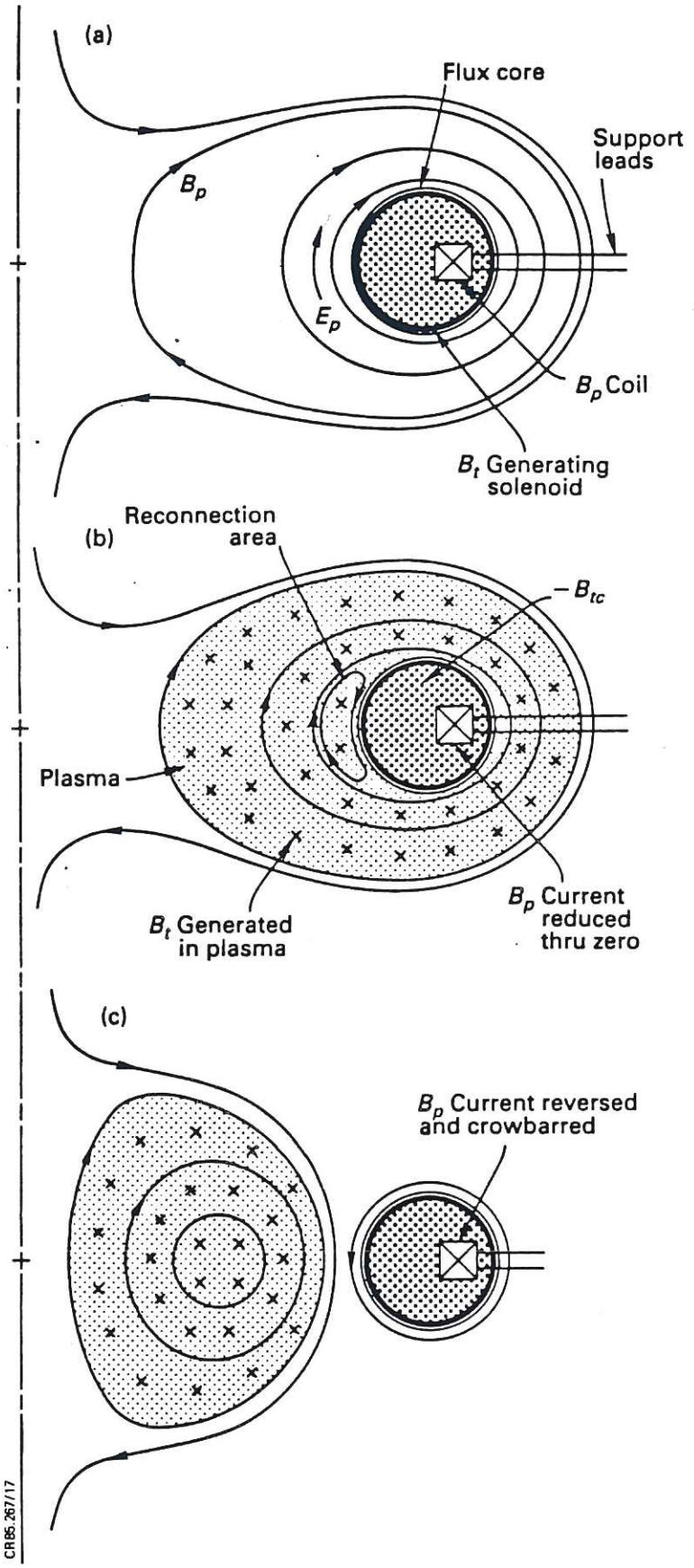

FIG. 17. Spheromak formation by inductive flux core (S-1).

(From Yamada et al., 1981.)

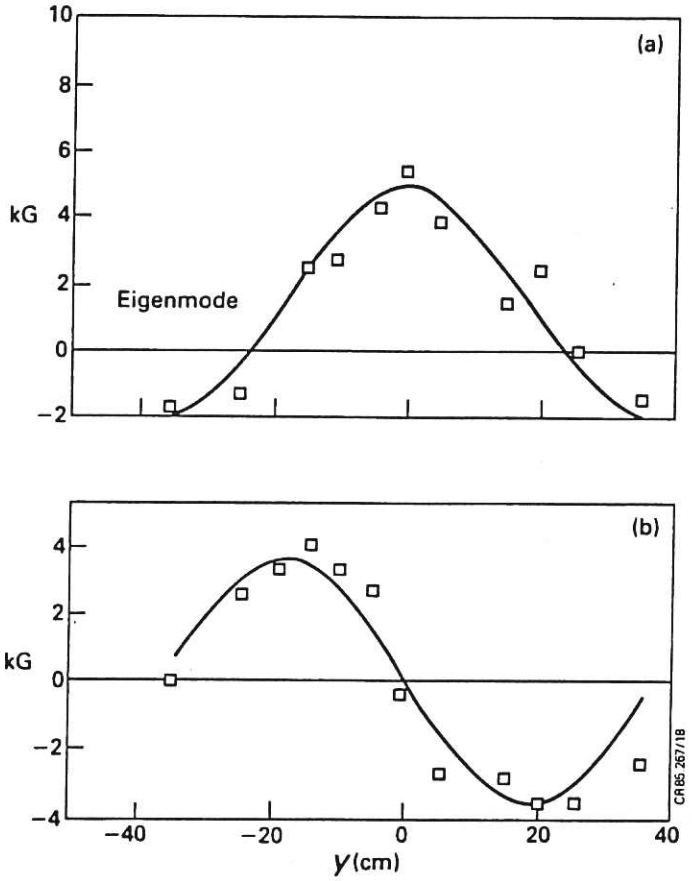

FIG. 18. Magnetic field in BETA II Spheromak. Experiment and theory. (a) Poloidal Field. (b) Toroidal Field. (From Turner et al., 1983.)

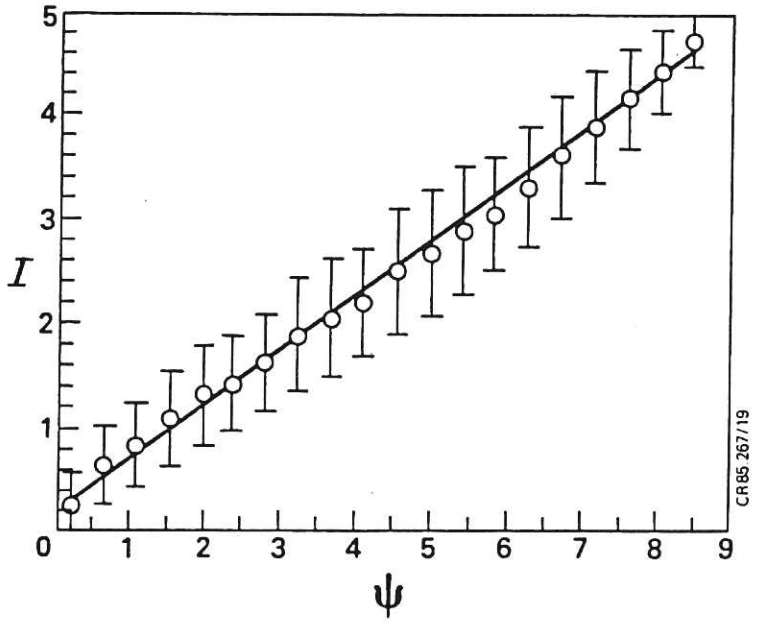

FIG. 19. Poloidal current vs. poloidal flux in Spheromak (S-1). (From Hart et al., 1985.)

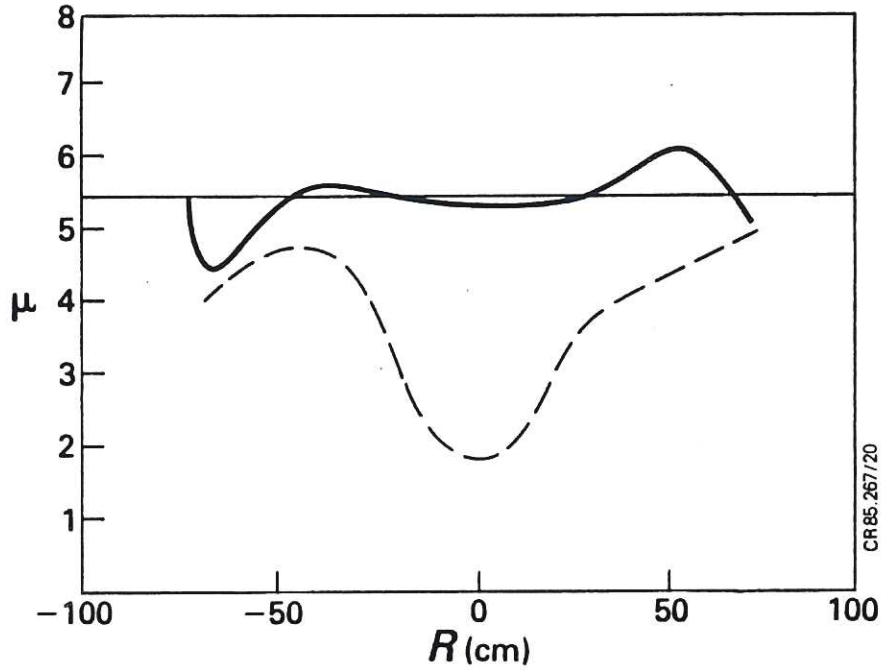

FIG. 20. Measured profile of $\mu(r)$ for Spheromak (S-1). (From Hart et al., 1985.)

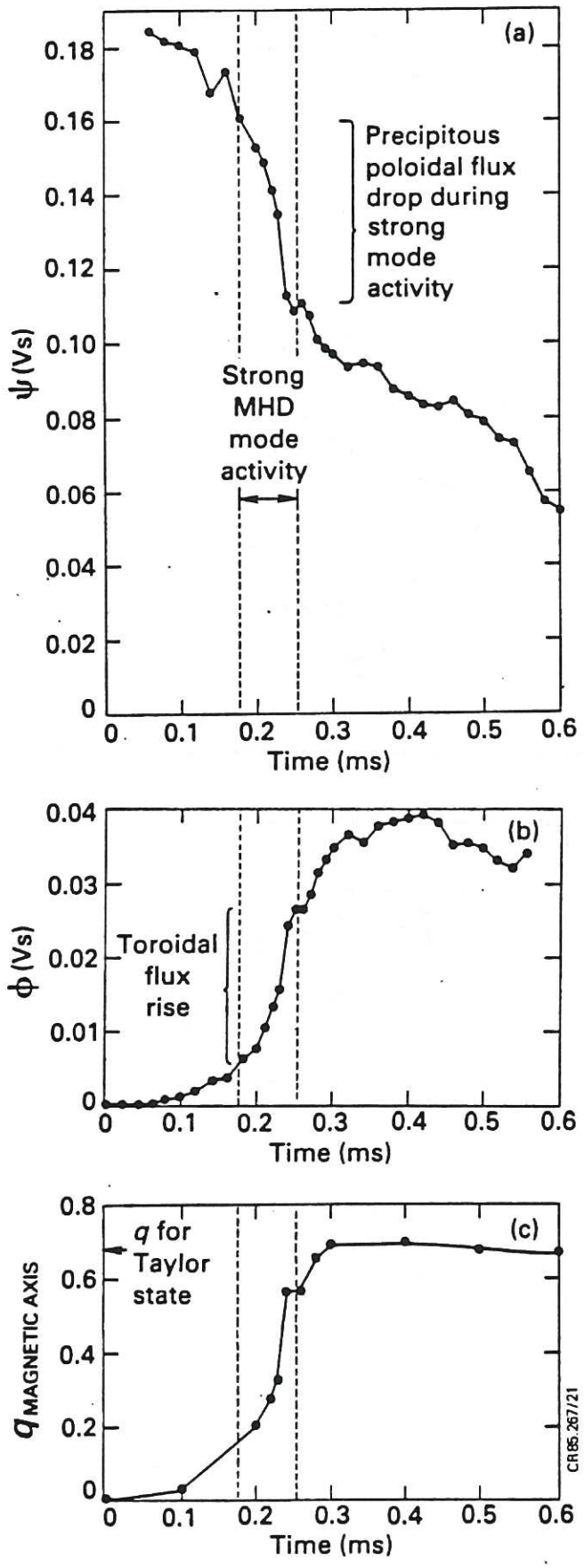

FIG. 21. Time dependence of magnetic fields in S-1 Spheromak. (From Janos et al., 1985.)

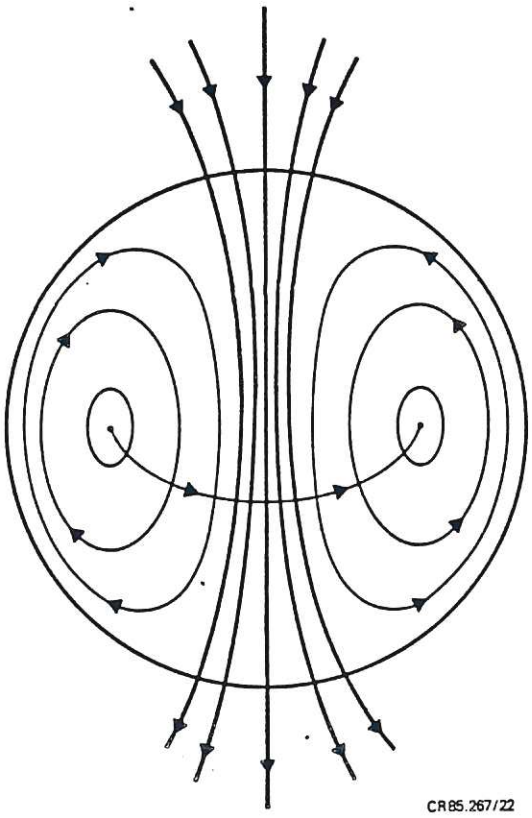

FIG. 22. Flux core Spheromak. Schematic.

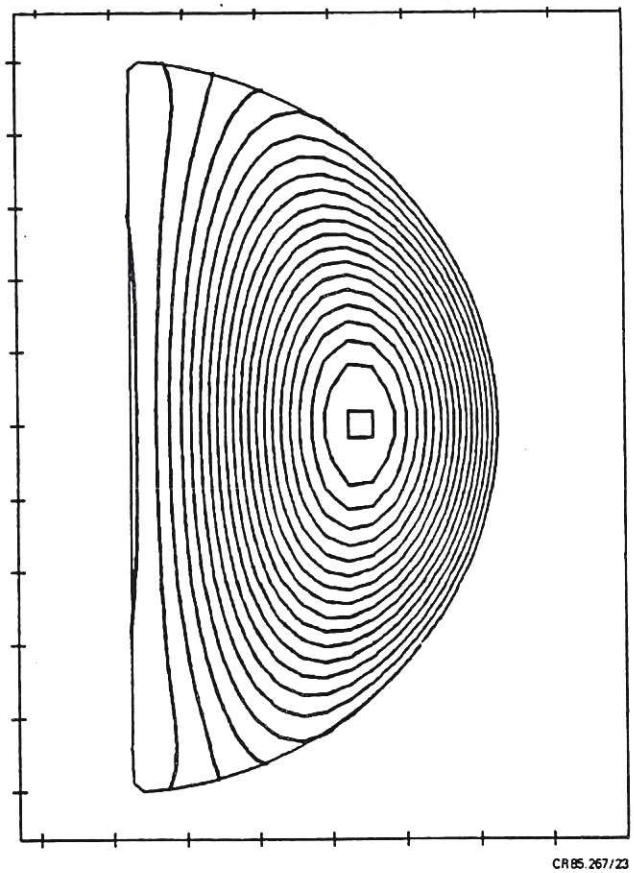

FIG. 23. Computed field in flux core Spheromak.

$\mu a = 4.09$.

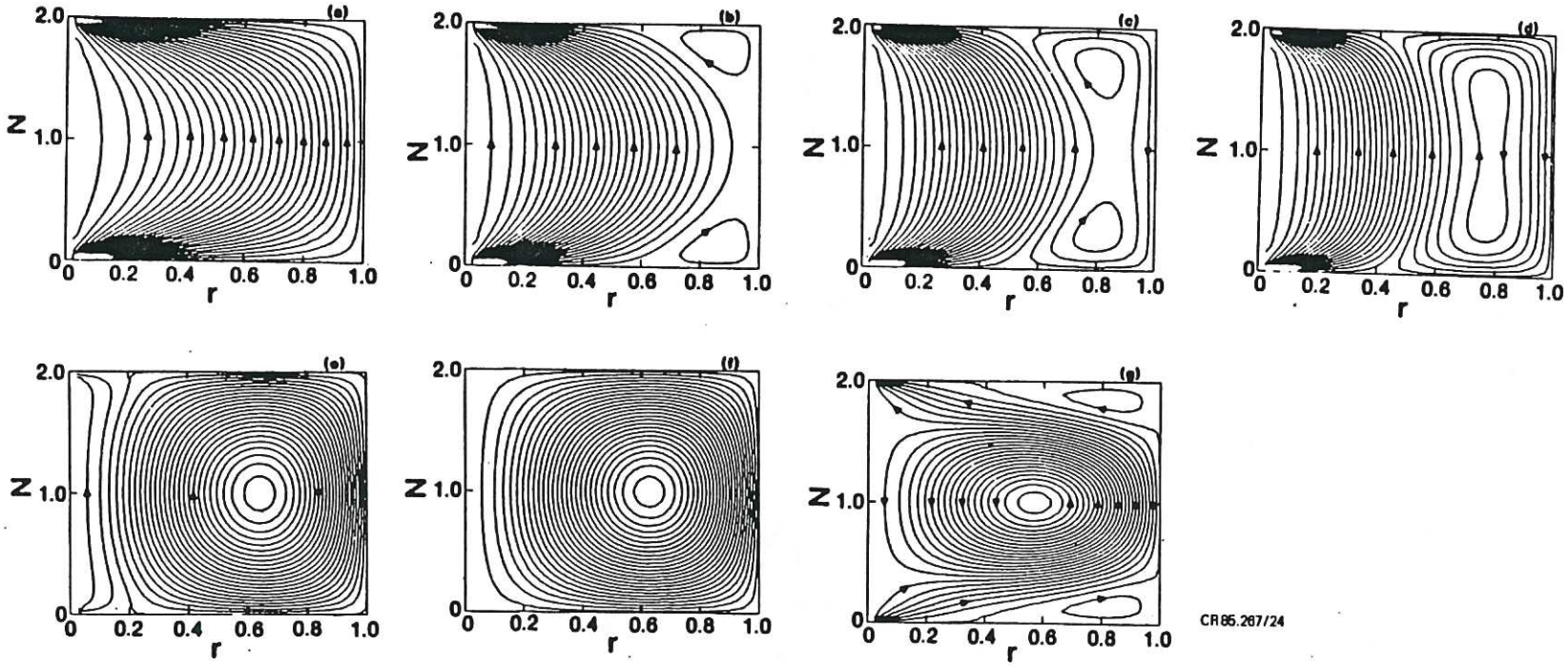

FIG. 24. Field in idealised FCS (vanishing polar cap radius) at various values of μa: (a) $\mu a = .001$, (b) $\mu a = 2.25$, (c) $\mu a = 2.70$, (d) $\mu a = 3.00$, (e) $\mu a = 4.00$, (f) $\mu a = 4.14$, (g) $\mu a = 5.00$. (From Turner, 1984.)

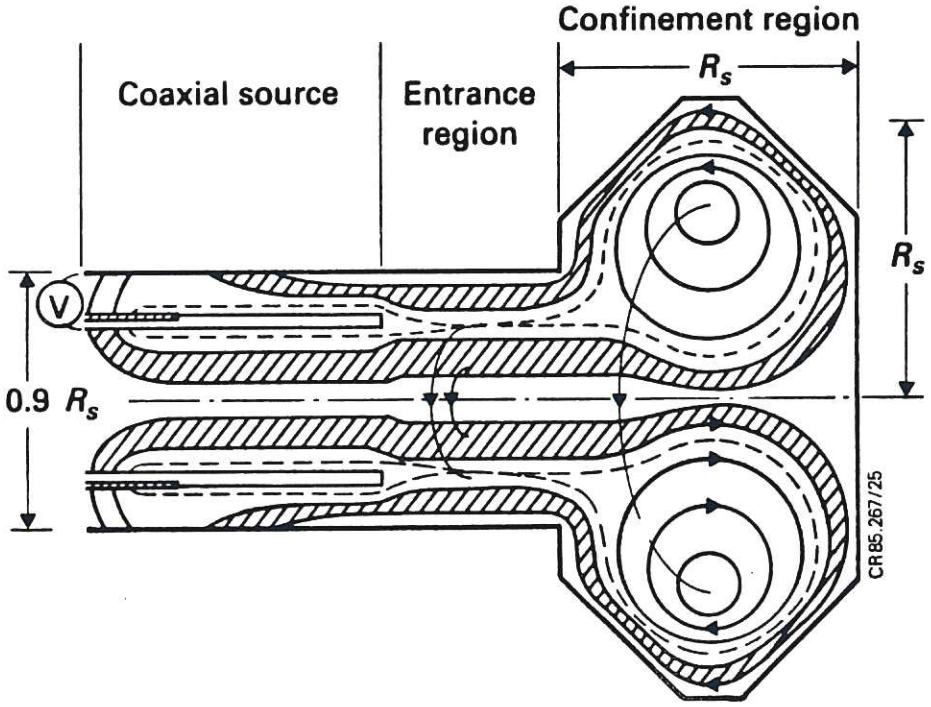

FIG. 25. Sustained configuration in CTX experiment.

(From Jarboe, 1985.)

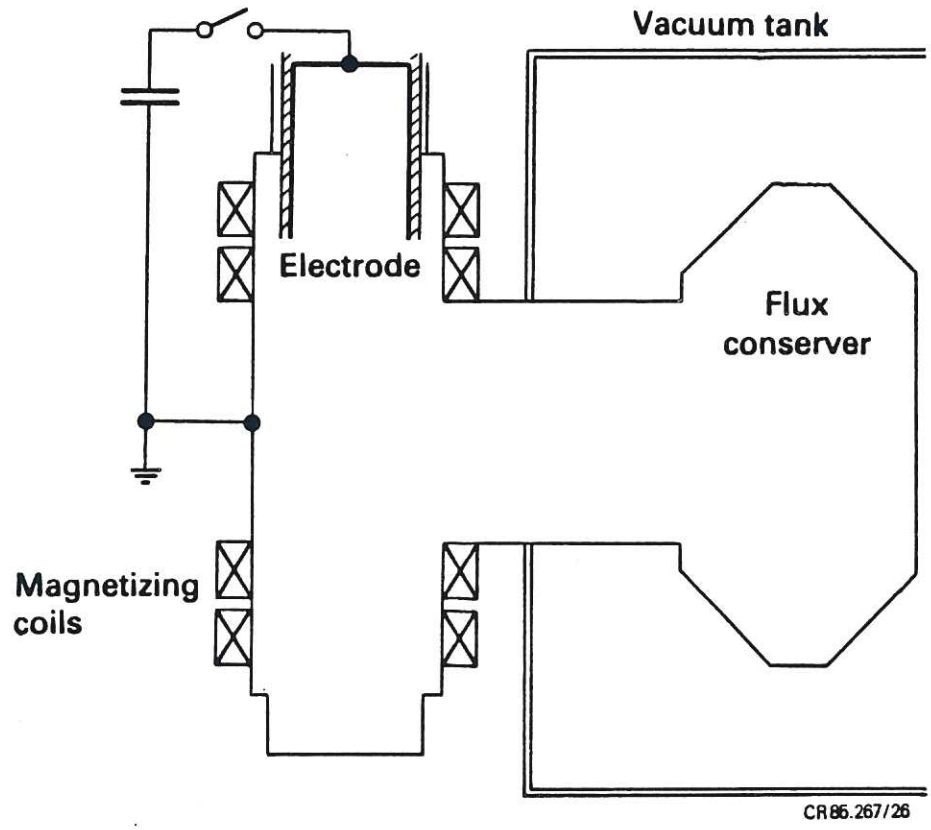

Kinked Z-pinch helicity source

FIG. 26. Experiment with remote helicity injection.

(From Jarboe, 1985.)